Palaeogeography, Palaeoclimatology, Palaeoecology 307 (2011) 75–89

Contents lists available at ScienceDirect

Palaeogeography, Palaeoclimatology, Palaeoecology

journal homepage: www.elsevier.com/locate/palaeo

Paleosol carbonates from the Omo Group: Isotopic records of local and regional environmental change in East Africa

Naomi E. Levin [a,b,*], Francis H. Brown [b], Anna K. Behrensmeyer [c], René Bobe [d], Thure E. Cerling [b]

[a] Department of Earth & Planetary Sciences, Johns Hopkins University, 3400 N. Charles Street, 301 Olin Hall, Baltimore MD 21218, USA
[b] Department of Geology & Geophysics, University of Utah, 115 S. 1460 East, Room 383, Salt Lake City UT, 84112, USA
[c] Department of Paleobiology, National Museum of Natural History, Smithsonian Institution, Washington, D.C., 20013, USA
[d] Department of Anthropology, University of Georgia, 265B Baldwin Hall, Jackson Street, Athens, Georgia 30602-1619, USA

ARTICLE INFO

Article history:
Received 25 October 2010
Received in revised form 18 April 2011
Accepted 23 April 2011
Available online 3 May 2011

Keywords:
Pedogenic carbonate
Omo–Turkana Basin
East Africa
Pleistocene
Pliocene
Carbon isotopes
Oxygen isotopes

ABSTRACT

Pliocene and Pleistocene sedimentary rocks from the Omo–Turkana Basin in East Africa are well known for fossil and archeological evidence of human evolution and provide a unique opportunity to study four million years of environmental change in a rift basin. This study uses carbon and oxygen isotope ratios of pedogenic carbonates to examine environmental variability across ~5000 km^2 within the Omo–Turkana Basin. An expanded isotopic dataset, including the first isotopic data on pedogenic carbonates from the Shungura Formation and new data from the Nachukui and Koobi Fora formations, is compared to published isotopic records from both the Omo–Turkana Basin and the lower Awash Basin, Ethiopia. Regionally, the carbon isotope record indicates a steady increase of C_4 vegetation in floodplain environments for the past 4 million years. The oxygen isotopic record indicates that the isotopic composition of rainfall was depleted in ^{18}O relative to today's waters and that both basins likely received more rainfall in the Pliocene than today. A shift to higher $\delta^{18}O$ values in paleosol carbonate after 2 Ma in the Omo–Turkana Basin but not in the lower Awash Basin suggests that the ecology and hydrology in these two rift basins were influenced by different climatic regimes. In addition to regional trends, pedogenic carbonates sampled from different parts of the basin show that the distribution of C_4 vegetation and soil water $\delta^{18}O$ values varied with proximity to the axial river system, and specifically that C_3 vegetation was more dominant in soils of the Shungura Formation compared with coeval sediments downstream in the Nachukui and Koobi Fora formations. This large isotopic dataset from pedogenic carbonates provides the opportunity to examine how terrestrial systems responded to global climate change during the last 4 million years, from both local and regional perspectives. The isotopic data indicate that local basin and climate dynamics strongly influenced the impact of large-scale environmental change in East African rift basins.

1. Introduction

Major events such as the onset and intensification of northern hemisphere glaciation, orbital shifts, and closure of Central American and Indonesian seaways, have significantly modified global climate since the Pliocene (Imbrie et al., 1992; Chaisson, 2000; Cane and Molnar, 2001; Haug et al., 2001). Dust and isotopic biomarker records from the Gulf of Aden and the Arabian Sea suggest that increased aridity and the greater abundance of C_4 vegetation (primarily warm growing season grasses and sedges) in East Africa are synchronous with trends in global climate during the Pliocene and Pleistocene (deMenocal, 2004; Feakins et al., 2005) and coincide with tectonic and topographic changes in East Africa that changed regional circulation (Sepulchre et al., 2006; Gani et al., 2007). Several recent terrestrial records also demonstrate links between East African environmental conditions and global-scale climate cycles since the Pliocene (McDougall et al., 2005; Deino et al., 2006; Ashley, 2007; Feakins et al., 2007; Lepre et al., 2007; Trauth et al., 2007).

Exposures of carbonate-rich paleosols throughout the lower Omo River Valley and the Turkana Basin provide an opportunity to examine basin-wide environmental responses to climate change during the Pliocene and Pleistocene. Here, new isotopic data from Omo Group paleosol carbonates are presented and document systematic environmental variability within the Omo–Turkana Basin during the past 4 million years. Comparison with existing isotopic data from the Omo–Turkana Basin and with coeval records in the lower Awash Basin in Ethiopia, 800 km northeast of the Omo–Turkana Basin, provides perspective on the local and regional scales of environmental variability in East Africa during the Pliocene and Pleistocene.

* Corresponding author. Department of Earth & Planetary Sciences, Johns Hopkins University, 3400 N. Charles Street, 301 Olin Hall, Baltimore MD 21218, USA. Tel.: +1 410 516 4317; fax: +1 410 516 4933.
E-mail address: nlevin3@jhu.edu (N.E. Levin).

0031-0182/$ – see front matter © 2011 Elsevier B.V. All rights reserved.
doi:10.1016/j.palaeo.2011.04.026

1.1. Study area

The Omo–Turkana Basin, in northern Kenya and southern Ethiopia, contains extensive exposures of Pliocene and Pleistocene sedimentary rocks known as the Omo Group (de Heinzelin, 1983), which fill a depression where the Main Ethiopian and East African rift systems meet (Fig. 1). The drive to build paleoenvironmental records from these rocks has been fueled by interests in establishing the context for human evolution (Leakey and Leakey, 1978; Brown et al., 1985; Howell et al., 1987). Well-dated and laterally extensive tephra link the Omo Group strata to one another and permit the basin-wide examination of a single depositional system (Fig. 2).

Sediment and water from the Ethiopian Highlands are the source for the majority of the Omo Group deposits. This makes deposition in the Omo–Turkana Basin dependent on tectonics of the Ethiopian highlands, water supply to the Omo River catchment, and local tectonic and volcanic activity that affect basin geometry (Brown and Feibel, 1991; Bruhn et al., 2011). The Omo River has flowed from the Ethiopian highlands into the Turkana Basin for at least five million years. The amount of Omo River water that entered and transited the Turkana Basin over this interval depended on rainfall in the Ethiopian highlands and stream diversion from the Omo River basin into the Nile (Brown and Feibel, 1991). The varying modes of deposition of Omo Group deposits are related to their location, either proximate to the Omo River, or proximate to the eastern or western margins of basin (Fig. 3).

The Omo Group deposits include the Shungura, Koobi Fora, and Nachukui formations, which have a cumulative thickness of 560–760 m and represent near-continuous deposition near the basin center between 4.3 and 0.6 Ma (Feibel et al., 1989). Shungura Formation strata, exposed today in the lower Omo River Valley in Ethiopia (Fig. 1), are dominated by fluvial deposition by the axial river system, the ancestral Omo River, which flowed south from the Ethiopian highlands into the Turkana Basin (de Heinzelin, 1983) (Fig. 3). South of the Shungura Formation, strata of the Koobi Fora and Nachukui formations are exposed east and west of Lake Turkana, respectively, and contain fluvial, deltaic, and lacustrine deposits. Various depositional modes characterize the Koobi Fora Formation and include fluvial deposition from the axial Omo River system and from smaller river systems draining the basin's eastern margin (the ramp side of the half-graben), extensive lake deposits, and deltaic sequences (Brown and Feibel, 1991). Closer to the western margin of the Turkana Basin, the Nachukui Formation is marked by abrupt variation in facies over short horizontal distances, where structural control on the western edge of the basin (the faulted margin of the half-graben) places lacustrine environments, high-energy shorelines, alluvial conglomerates and axial river deposits very close to one another (Harris et al., 1988).

Broad floodplains adjacent to the ancestral Omo River and interfluves between alluvial systems produced a landscape that was conducive to soil development. Cerling (1986) estimated that annually the Omo River transported $10–20 \times 10^{12}$ g of sediment to the Turkana Basin. Periodic rapid addition of new sediment to active floodplains would regularly quench soil development, seal the interval that each soil records, and provide the substrate for the next pedogenic interval. The cyclic nature of deposition created stacks of soils that provide snapshots (10^3–10^5 years duration) of floodplain environments through time.

1.2. Paleosols

Paleosols have been used previously as indicators of climate, vegetation and depositional mode in the Omo–Turkana Basin (Haesaerts et al., 1983; Cerling et al., 1988; Wynn, 2000, 2004; Quinn et al., 2007). Floodplain paleosols occur throughout the alluvial and fluvial deposits of the Omo Group (Haesaerts et al., 1983; Brown and Feibel, 1991; Feibel et al., 1991). Many of these paleosols are Vertisols, which are smectite-rich, shrink-swell soils that form in arid to semiarid, highly seasonal climates (Ahmad, 1983; Feibel et al., 1991). Parent material in the Omo Group calcic Vertisols is volcanic or crystalline basement rock from calcium-rich source areas and is generally free of carbonate. Carbonate-rich soils form in seasonally

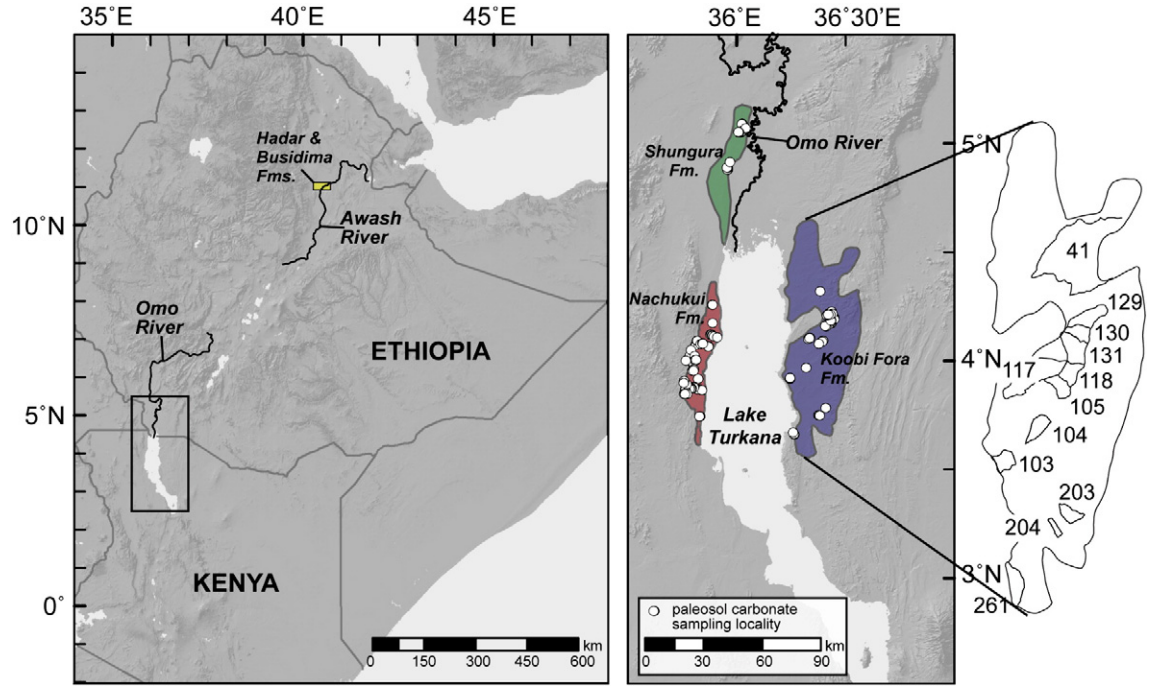

Fig. 1. Digital elevation map (DEM) of East Africa with locations of sites and geographic features discussed in text. The inset map provides a detail of the northern part of the Turkana Basin and the lower Omo River Valley. The extent of each formation in the Omo Group deposits is outlined. Filled circles mark locations of pedogenic carbonates sampled for this study. A close-up of the Koobi Fora Formation shows collection areas from which pedogenic carbonates were sampled.

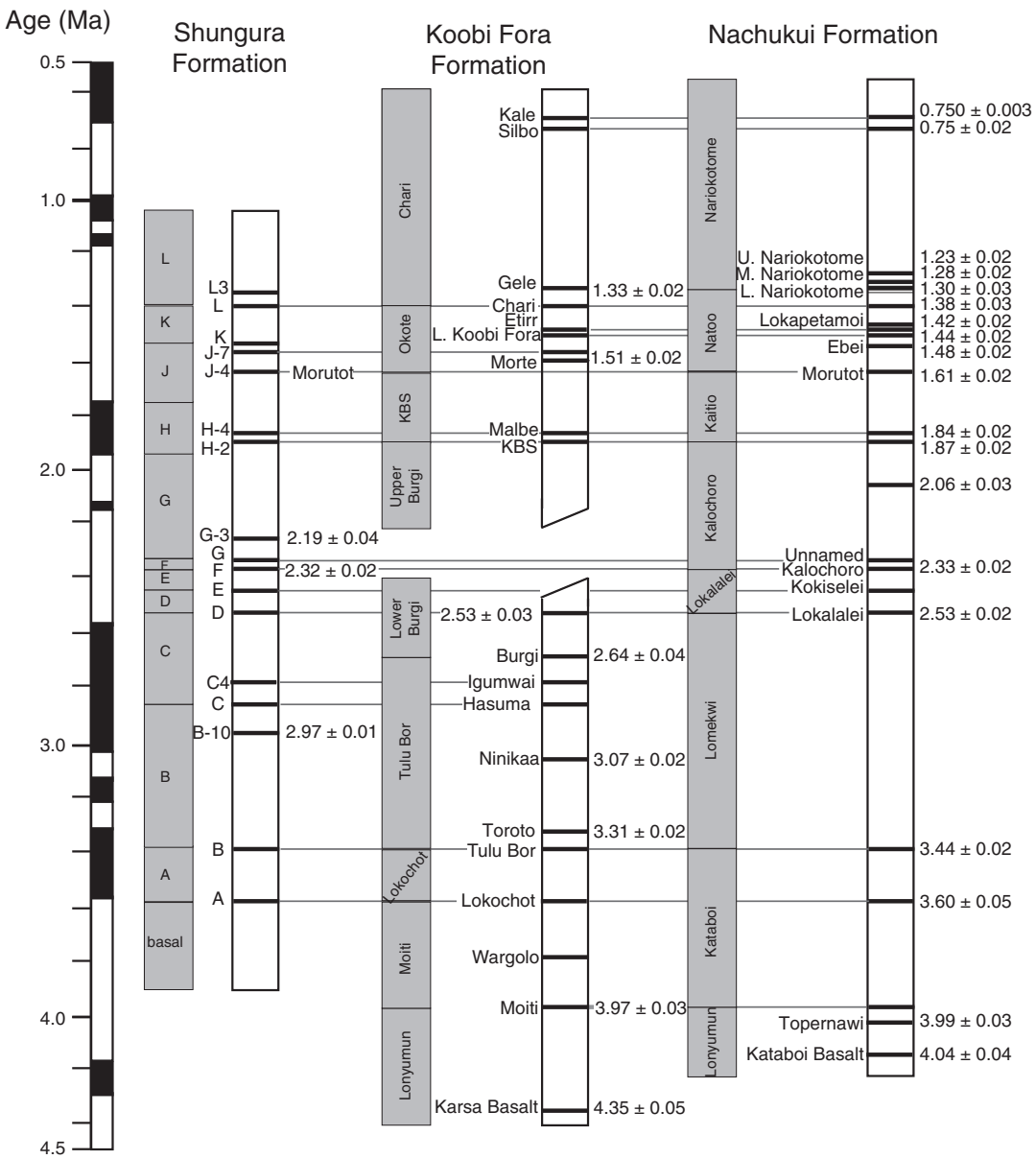

Fig. 2. Formations, members and major tuffs from the Omo Group. Isotope chronology (ages listed in Ma) and tephra correlations are based on Brown et al. (1992), Katoh et al. (2000), WoldeGabriel et al. (2005), Brown et al. (2006), McDougall and Brown (2006, 2008). Tephra correlations are marked by solid lines within and between sections. The geomagnetic polarity time scale is listed for reference (Cande and Kent, 1995). Members of each formation are indicated in gray blocks, based on Feibel et al. (1989).

dry environments that receive <1 m of rainfall annually and can take 10^2–10^5 years to form (Jenny, 1980; Machette, 1985; Retallack, 2005). Carbonate precipitation may occur in soils by a combination of soil dewatering by plants, evaporation, decreases in soil CO_2 concentration, and temperature changes that affect calcite solubility (Machette, 1985; Breecker et al., 2009; Passey et al., 2010). During the interval of carbonate formation, the carbon and oxygen isotope composition of soil CO_2 and soil water influence the isotopic composition of pedogenic carbonates. The isotopic composition of pedogenic carbonate can in turn be used as a proxy for local vegetation and hydrological conditions.

1.2.1. Pedogenic carbonate $\delta^{13}C$

Plants may be placed into three categories that represent different photosynthetic pathways: C_3, C_4 and Crassulacean Acid Metabolism (CAM). In East Africa, the majority of shrubs and trees use the C_3 pathway, whereas lower elevation (<3000 m) grasses use the C_4 pathway (Tieszen et al., 1979; Young and Young, 1983). Plants that use the CAM pathway include cacti, succulents, orchids and bromeliads (Lambers et al., 2008). As it is unlikely that such plants contribute a large proportion of biomass to the floodplain environments studied here, they are not considered further. Carbon isotope ratios ($^{13}C/^{12}C$) of pedogenic carbonates can be used to determine the proportion of C_3 and C_4 plants growing in soils because (1) C_3 and C_4 plants have distinct carbon isotopic signatures, (2) under high plant productivity and at depth in the soil (>40 cm), soil CO_2 reflects the ^{13}C composition of plants growing in soils, and (3) $^{13}C/^{12}C$ ratios of carbonates formed in equilibrium with soil CO_2 incorporates the carbon isotope ratio of soil CO_2 (Cerling and Quade, 1993). Stable carbon isotope ratios are reported relative to the isotopic standard Vienna Pee Dee Belemnite (VPDB) and presented as δ-values in per mil (‰) units, where $\delta^{13}C = [(^{13}C/^{12}C)_{sample}/(^{13}C/^{12}C)_{standard} - 1] * 1000‰$. $\delta^{13}C$ values of C_3 plants average $-31.4 \pm 0.5‰$, $-27.8 \pm 0.5‰$ and $-27.0 \pm 0.2‰$ in closed canopy forests, open canopy forests and savanna and bushland environments respectively, whereas $\delta^{13}C$ values of C_4 grasses range from $-11.8 \pm 0.2‰$ to $-13.1 \pm 0.2‰$ for

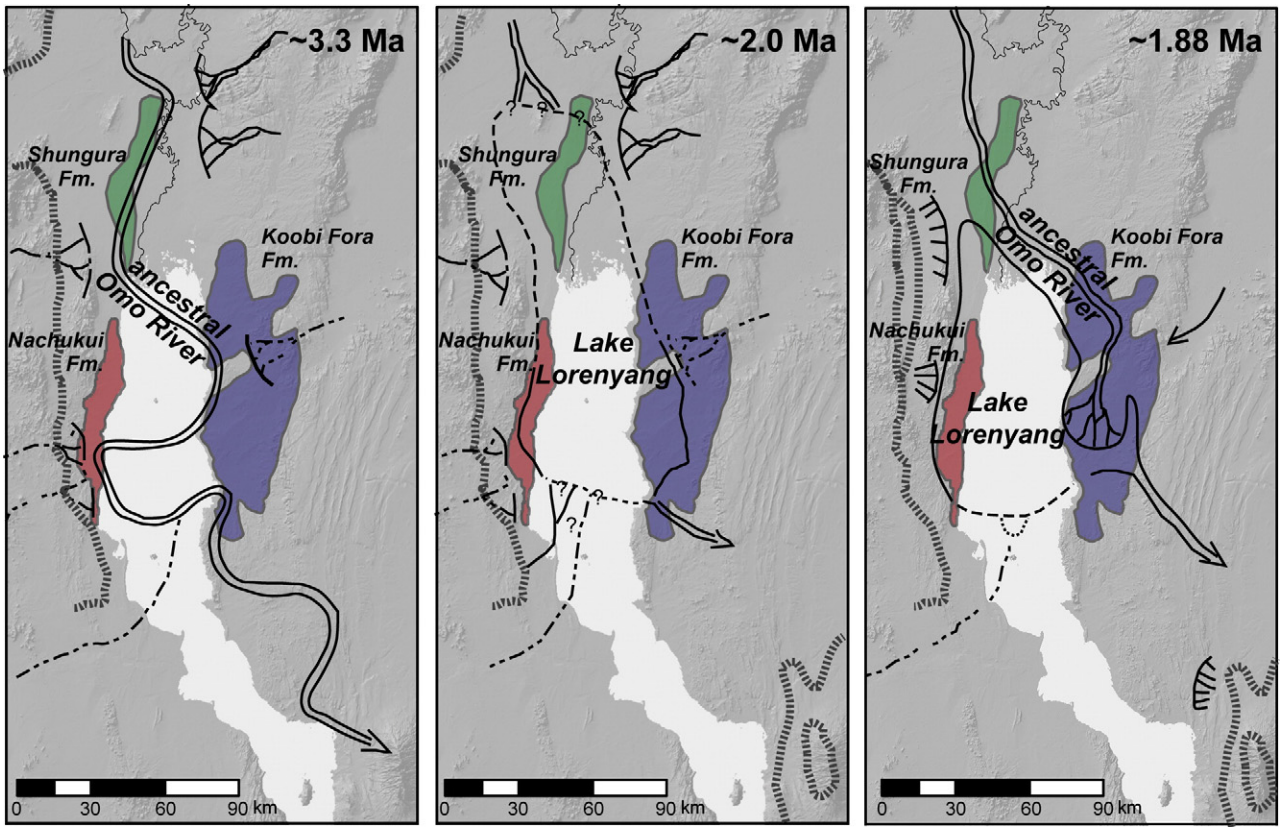

Fig. 3. Paleogeographic representations of the depositional settings and sedimentary environments of the Omo–Turkana Basin at approximately 3.3 Ma, 2.0 Ma and 1.88 Ma based on Brown and Feibel (1991), with positions of volcanic highlands (hashes) axial fluvial deposits (solid and dashed lines), alluvial fans (curved lines adjacent to shorter perpendicular lines) and major lakes (e.g. Lake Lorenyang) marked and overlain on a DEM of the region with the current distribution of exposed Omo Group strata as in Fig. 1.

mesic- and xeric-adapted forms (Cerling et al., 2003). Variation in $\delta^{13}C$ values for both C_3 and C_4 plants can be a function of water stress, light availability and canopy position (Farquhar et al., 1989; van der Merwe, 1991; Cerling et al., 2003).

$\delta^{13}C$ values of pedogenic carbonates ($\delta^{13}C_{pc}$) can be used to determine the proportion of C_4 to C_3 biomass growing in the soil for the duration of pedogenic carbonate formation (Cerling and Quade, 1993). In soils where plant productivity is high (>3–5 mmol $CO_2/m^2/h$), carbonates form in equilibrium with plant-derived soil CO_2 that is not mixed with atmospheric CO_2 (Cerling, 1999). The carbon isotope enrichment factor between plant derived CO_2 and pedogenic carbonate depends on a combination of kinetic and equilibrium fractionation processes. Diffusion of ^{13}C-depeted CO_2 in soils is a kinetic process that leaves the remaining soil CO_2 enriched in ^{13}C relative to ^{12}C by 4.4‰ or greater (Cerling et al., 1991; Davidson, 1995). Temperature-dependent equilibrium exchange between dissolved carbon species and plant-derived CO_2 results in carbonate enriched in ^{13}C by 9.6–7.8‰ relative to soil CO_2 for temperatures between 20 and 35 °C (Romanek et al., 1992), which includes the range of mean annual temperature (MAT) for regions in Kenya today (East African Meteorological Department, 1975) and mean soil temperatures (>50 cm depth) for Turkana (Passey et al., 2010). Considering the combined effects of kinetic and equilibrium fractionation, the carbon isotope enrichment between plants and pedogenic carbonates should be approximately 12–14‰ under high soil respiration rates and 14–17‰ for low respiration rates.

1.2.2. Pedogenic carbonate $\delta^{18}O$

$\delta^{18}O$ values of pedogenic carbonates ($\delta^{18}O_{pc}$) are determined by the oxygen isotopic composition of soil water and soil temperature, wherein soil water $\delta^{18}O$ is determined by $\delta^{18}O$ of rainfall and the degree of soil water evaporation. Rainfall feeds soil water through infiltration during precipitation events and surface run-off such that the $\delta^{18}O$ value of the resultant soil water may be a mixture of rainfall representing averages of specific precipitation events and accumulations over the course of seasons (Breecker et al., 2009). $\delta^{18}O$ values of rainfall vary with climate. In tropical regions like East Africa, rainfall amount, elevation and moisture source are the prime determinants of rainfall $\delta^{18}O$ values (Dansgaard, 1964; Rozanski et al., 1996; Levin et al., 2009). Surface water is subject to evaporation before and after it enters a soil such that remaining soil water can be enriched in ^{18}O because molecules of $H_2^{16}O$ are lost to the vapor phase in preference over $H_2^{18}O$ molecules (Craig and Gordon, 1965). Reflecting the effects of evaporation, $\delta^{18}O_{pc}$ values are often highest at the surface, where the potential for soil water evaporation is greatest (Quade et al., 1989; Barnes and Turner, 1998; Hsieh et al., 1998; Breecker et al., 2009). $\delta^{18}O_{pc}$ values are also a function soil temperature because the ^{18}O fractionation between water and carbonate is temperature dependent (−0.2‰/°C) (Kim and O'Neil, 1997). Measurements of soil temperatures in the Turkana Basin today indicate significant solar heating such that for most of the year (August–May) they average 35.2 ± 1.6 °C at 50 cm depth, exceeding the MAT of 29 °C (Passey et al., 2010).

1.3. Existing pedogenic carbonate records

Pedogenic carbonate isotope records have been used to assess the terrestrial response to global climate change (Cerling, 1992; Quade and Cerling, 1995; Amundson et al., 1996). In East Africa, such records document both local ecological variability and regional environmental changes, such as the expansion of grasslands and increased aridity in East Africa through the Pliocene and Pleistocene (Cerling et al., 1988;

Wynn, 2000; Levin et al., 2004; Wynn, 2004; Quinn et al., 2007; Sikes and Ashley, 2007).

The paleosol isotope record from the Koobi Fora Formation by Cerling et al. (1988) was the first of its kind for the Omo–Turkana Basin and showed that C_4 grasses did not become well established in floodplain regions until 1.8 Ma. Cerling and colleagues attribute the relative abundance of C_3 vegetation before 1.8 Ma to a preservation bias towards riparian woodlands on the floodplain of the ancestral Omo River. In his synthesis of $\delta^{13}C_{pc}$ values from Kanapoi, the Nachukui Formation and the Koobi Fora Formation, Wynn (2004) also identifies an increase in C_4 biomass through time in both the eastern and western parts of the Turkana Basin. Quinn et al. (2007) present a detailed $\delta^{13}C_{pc}$ record for the Koobi Fora Formation in the 2.0–1.5 Ma interval and show a pronounced increase in $\delta^{13}C_{pc}$ values after 1.8 Ma in some regions (Koobi Fora Ridge) but not in others (Karari Ridge).

The $\delta^{18}O_{pc}$ record from Turkana paleosols has been interpreted as an indicator of climate change and basin dynamics. Cerling et al. (1988) document an increase in $\delta^{18}O_{pc}$ values from the Koobi Fora Formation after deposition of the KBS Tuff, which could be due to an increase in rainwater $\delta^{18}O$ values, increased aridity, or a change in basin hydrology. Similar shifts in rainfall $\delta^{18}O$ values in East Africa have also been inferred from $\delta^{18}O_{pc}$ records from Plio-Pleistocene deposits elsewhere in Kenya and in Ethiopia (Hillaire-Marcel et al., 1982; Hailemichael et al., 2002; Levin et al., 2004; Liutkus, et al., 2005; Sikes and Ashley, 2007). There is no discussion of $\delta^{18}O_{pc}$ values in the detailed sampling of the Koobi Fora Formation by Quinn et al. (2007) and only a brief discussion of $\delta^{18}O_{pc}$ values from the Nachukui Formation by Wynn (2004). A recent study using carbonate clumped isotope thermometry on pedogenic carbonate from the Shungura and Nachukui formations shows that most paleosol carbonates from the Omo Group, regardless of age or basin position, formed in soils that on average were hotter than 30 °C, showing that throughout the Pliocene and Pleistocene the Omo–Turkana Basin was as hot as or hotter than it is today (Passey et al., 2010).

Despite multiple pedogenic carbonate records from the Omo Group, previous isotopic data are still insufficient to evaluate the environmental diversity across this large basin during the last 4 million years. The data presented in this paper expand on the existing isotopic record from paleosols by filling temporal gaps, adding data from the Shungura Formation, and systematically sampling synchronous intervals across the basin to document lateral environmental gradients.

2. Materials and methods

Paleosol carbonate samples were placed into the Omo Group stratigraphy based on position with respect to tephra marker horizons that have been geochemically correlated throughout the basin (e.g., Brown et al., 2006; McDougall and Brown, 2008). The sampling strategy was designed to generate isotopic records in previously unsampled portions of the basin (e.g., Shungura Formation) and complement existing paleosol carbonate isotope records by extending their temporal and spatial range.

As previously observed and discussed (Haesaerts et al., 1983; Feibel, 1988; Brown and Feibel, 1991; Quinn et al., 2007), the majority of paleosols in the Omo–Turkana Basin formed in fine-grained sediments at the tops of fining upward fluvial sequences. Most paleosols sampled for this study are vertic, dark brown and characterized by the down-profile increase of clay content, carbonate content, slickensided ped surfaces, blocky structure, and minor Mn and Fe oxides on slickensided surfaces. Some of the paleosols have minor green and gray mottling, or sand filled cracks, whereas others have distinct prismatic soil structure (Feibel, 1988). The parent material for most Omo Group paleosols is non-calcareous fine silt or clay, but some paleosols developed on sands and gravels. Mature soils were recognized by increased down-profile clay development, distinct horizonation, dish-shaped crack structures and fractures, and higher carbonate concentrations in the Bk horizon. The majority of calcareous Vertisols from the Omo Group have Stage I or Stage II carbonate development (Machette, 1985).

Nodular paleosol carbonates were collected from carbonate (Bk) horizons at least 40 cm below the upper boundary of the paleosol in order to avoid the influence of ^{13}C-enriched atmospheric CO_2 on carbonate $\delta^{13}C$ values, although mechanical mixing of nodules vertically within the soil profile does occur in Vertisols (Nordt et al., 2004). Only discrete nodular carbonate from a clear Bk horizon was sampled. Multiple nodules 0.2–2 cm in diameter were sampled for each paleosol pit dug (~1 m^2). Larger nodules, diffuse carbonate, rhizoliths, and carbonate filling in cracks between vertic dish structures were not included in this study. One to three nodules from each paleosol locality were prepared for carbon and oxygen isotope ratio measurements. Before analysis, nodule interiors were visually inspected with an optical microscope to ensure that they were micritic. Nodules were drilled with a diamond bit, avoiding detritus and mm-scale secondary calcite veins that cross cut many nodules.

Stable isotope ratios of pedogenic carbonates sampled for this study can be considered faithful recorders of $\delta^{13}C$ values of plant respired CO_2, soil temperature and soil water $\delta^{18}O$ values because (1) carbonates were sampled at depth in distinct Bk horizons, (2) carbonate samples come from Vertisols where vadose zone processes were dominant, (3) there are no signs of detrital carbonate in the soil parent material, and (4) there were no indications of postburial carbonate replacement or exchange in the micritic areas of the nodules where they were sampled.

Prior to isotopic analysis, powdered pedogenic carbonate was roasted under vacuum at 250–400 °C for 3 h. The powdered carbonate was then digested with silver capsules in 100% H_3PO_4 at 90 °C using an on-line carbonate device, the Finnigan Carboflo, and analyzed on a Finnigan MAT 252 gas-source mass spectrometer at the University of Utah. Corrections were based on Carrara marble used as laboratory standard and calibrated to the NBS-19 calcite standard. Precision (1σ) of the Carrara marble reference material was 0.07‰ and 0.09‰ for $\delta^{13}C$ and $\delta^{18}O$, respectively over the course of the analyses made for this study. Isotope ratios of some of the carbonates from the Koobi Fora Formation were measured at the University of Arizona, where they were digested in 100% H_3PO_4 at 90 °C using an on-line Kiel device. The isotope ratios of the resultant CO_2 were measured on a Finnigan MAT 252 gas-source mass spectrometer; the long-term precision (1σ) for $\delta^{13}C$ and $\delta^{18}O$ values of the reference material NBS-19 is 0.06‰ and 0.10‰, respectively. All isotope values from are reported in δ-notation in reference to the isotopic standard Vienna Pee Dee Belemnite (VPDB) and in reference to Vienna Standard Mean Ocean Water (VSMOW) for carbonates and waters respectively. Statistics were computed with the JMP® statistical software, Version 7, SAS Institute. Comparisons between samples were made with Wilcoxon rank-sum tests. Trends were identified using least squares linear regression and reported as the coefficient of determination, R^2. Correlations are reported as r, the Pearson correlation coefficient, at a 95% confidence density ellipse. If not otherwise specified, errors are reported as the standard deviation (1σ) of a mean.

Ages of paleosol carbonate samples were determined based on stratigraphic position relative to a dated marker horizon, assuming uniform sedimentation rates for the given member. Sedimentation rates were calculated for type sections of the members in each formation using the most recent chronology for the Omo Group tephra (McDougall and Brown, 2006, 2008). Twenty-seven dated units and 11 paleomagnetic polarity transitions within the Omo–Turkana Basin enable us to constrain the sampled paleosols to time intervals of 20–300 kyr (Fig. 2); the best dated paleosols come from lower Member G in the Shungura Formation where there are 13 paleosols within 260 thousand years (Fig. 4). These time intervals reflect our understanding of the absolute age of a paleosol; however

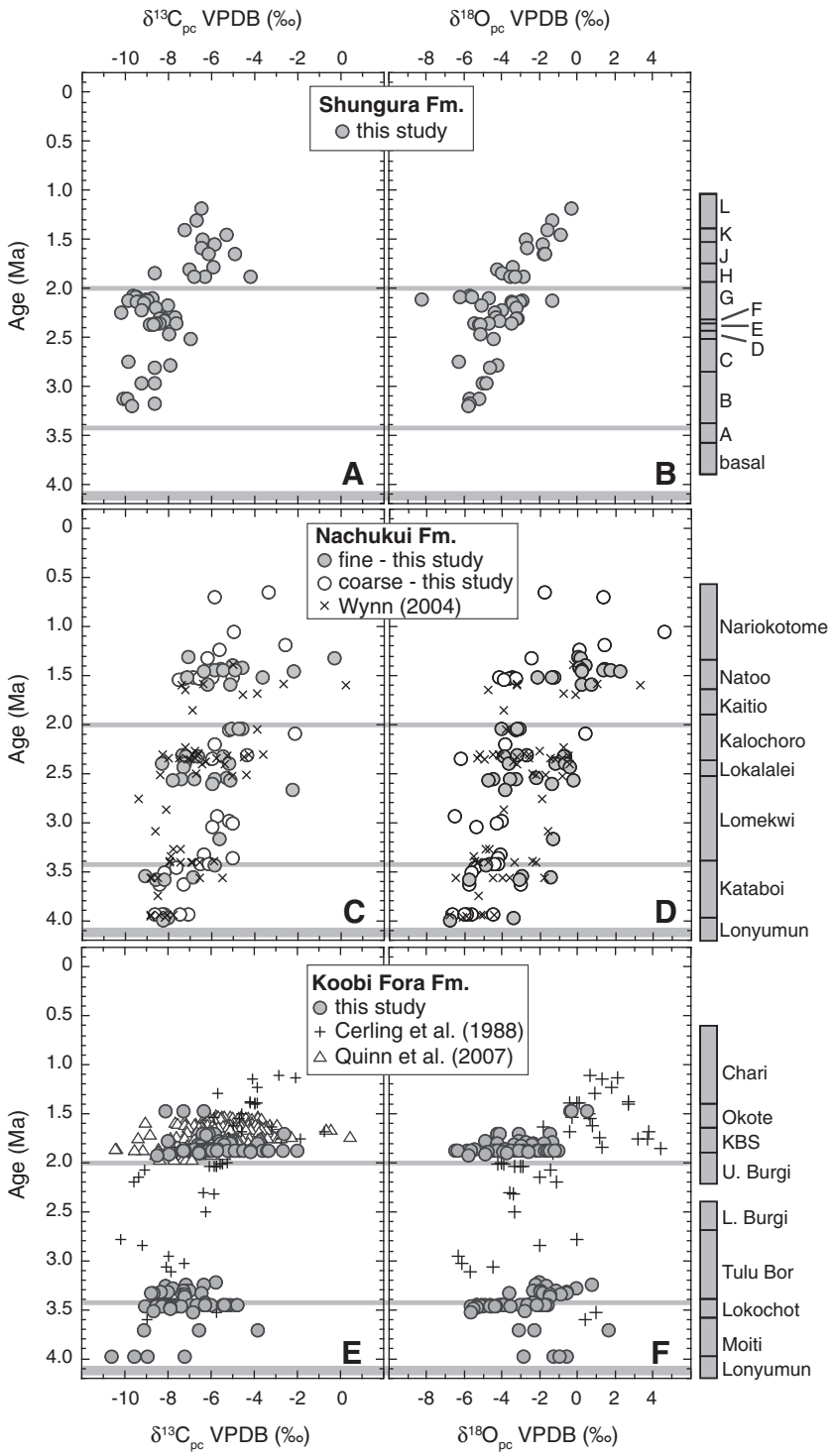

Fig. 4. $\delta^{13}C$ and $\delta^{18}O$ values of pedogenic carbonates (mean values for each paleosol sampled) from the Shungura Formation (A,B), the Nachukui Formation (C,D), and the Koobi Fora Formation (E,F). For the Nachukui Formation, results from this study are differentiated by their association with fine- or coarse-grained sediments. Results from previously published $\delta^{13}C$ and $\delta^{18}O$ values from the Nachukui and Koobi Fora formations are also plotted (Cerling et al., 1988; Wynn, 2004; Quinn et al., 2007). Members for each formation are listed to the right of each plot and basin-wide lacustrine intervals are marked with horizontal gray bars.

the duration of each soil-forming episode likely was much shorter than these outer limits and is likely <20 kyr. This estimate is supported by the small size (<2 cm diameter) of the sampled pedogenic carbonate nodules, which would predict pedogenic duration <8 kyr, based on regressions reported by Retallack (2005).

Interpretations of paleovegetation from $\delta^{13}C_{pc}$ values are made with consideration of the ~1.5‰ decrease in $\delta^{13}C$ values of atmospheric CO_2 ($CO_{2(atm)}$) in the last 150 years due to the Suess effect caused by burning of ^{13}C-depleted fossil fuels (Keeling et al., 1979; Francey et al., 1999). A compilation of $\delta^{13}C$ values of benthic foraminifera by Tipple et al. (2010) indicates that $CO_{2(atm)}\delta^{13}C$ values average -6.6 ± 0.54‰ ($n = 858$) during the last 4 million years, amidst a 1‰ decrease in $CO_{2(atm)}\delta^{13}C$ values from the early Pliocene to the pre-Industrial present. The magnitude of this decrease is too

small and the range in reconstructed $CO_{2(atm)}\delta^{13}C$ values at any given time period is too large to justify any systematic corrections for $CO_{2(atm)}\delta^{13}C$ values that would be meaningful for interpreting the $\delta^{13}C_{pc}$ data from this study.

3. Results

In the following sections, pedogenic carbonate isotope data from the Shungura, Nachukui and Koobi Fora formations are reported. General trends from each formation are presented and then discussed for specific time intervals. Data are discussed as the average isotopic values for a paleosol site (~1 m^2), not for each nodule analyzed. A full list of carbon and oxygen isotope ratio data is included in the Supplementary Data, Table 1.

3.1. Shungura Formation

Pedogenic nodular carbonate was sampled from 49 stratigraphic levels, between Members B and L in the Shungura Formation. All paleosols sampled from the Shungura Formation represent soil development on floodplains of the proto-Omo River (Haesaerts et al., 1983) (Fig. 3). For most of the sampled paleosols, two pedogenic carbonate nodules were analyzed. The range in isotopic composition of nodules from the same paleosol averaged 0.7 ± 0.7‰ and 1.5 ± 1.1‰ ($n=48$) for $\delta^{13}C$ and $\delta^{18}O$, respectively.

Pooled together from all time horizons in the Shungura Formation, $\delta^{13}C_{pc}$ values average −8.1 ± 1.5‰ ($n=49$) and range from −10.2 to −4.2‰ (Fig. 4). There is a marked increase in $\delta^{13}C_{pc}$ values after the retreat of the Lorenyang Lake and the return of fluvial deposition in Member H ($R^2=0.40$). Paleosols from strata older than the appearance of the Lorenyang Lake ~2.0 Ma (Member G and below) yield $\delta^{13}C_{pc}$ values that average −8.9 ± 0.8‰ ($n=34$), whereas paleosols in strata that postdate the lake (Member H and above) yield significantly different $\delta^{13}C_{pc}$ values ($p<0.0001$) that average −6.3 ± 1.0‰ ($n=15$). $\delta^{18}O_{pc}$ values from all paleosols sampled from the Shungura Formation average −4.0 ± 1.6‰ ($n=49$) and range from −8.3 to −0.3‰ (Fig. 4). The range in $\delta^{18}O_{pc}$ values (6.9‰) is greatest in sub Members G-5 through G-13 where sedimentation rates are high (~70 cm/kyr). There is a gradual increase in $\delta^{18}O_{pc}$ values from −5.8‰ at 3.20 Ma to −0.3‰ at 1.18 Ma ($R^2=0.47$). Paleosols stratigraphically below the Lorenyang Lake at the top of Member G yield $\delta^{18}O_{pc}$ values that are significantly lower than $\delta^{18}O_{pc}$ values from paleosols that appear after regression of the lake ($p=0.0007$).

3.2. Nachukui Formation

Pedogenic carbonates were sampled from 76 paleosols in the Nachukui Formation from the Lonyumun Member at the base of the sequence at 3.99 Ma upward through the Nariokotome Member at <0.75 Ma (Fig. 4). Temporal gaps in the record are due to the absence of calcareous paleosols or the inability to constrain the age of a sample in direct reference to a dated horizon. For example, few paleosols were sampled in the interval between 2.03 and 1.5 Ma when the region was dominated by lacustrine and lake margin facies (Fig. 3). Higher in the section in the Nariokotome Member, lack of exposures and chronologic control prevented sampling many paleosols younger than 1.2 Ma. Where possible, multiple paleosols were sampled at the same stratigraphic horizon (i.e., above or below a marker tuff unit). One to four carbonate nodules were analyzed for each paleosol locality. Among nodules sampled from the same paleosol site, the range in $\delta^{13}C$ values averaged 1.2 ± 1.3‰ and 0.7 ± 0.6‰ for $\delta^{18}O$ ($n=75$).

When data from all time intervals in the Nachukui Formation are grouped, $\delta^{13}C_{pc}$ values average −6.1 ± 1.7‰ and range from −9.1 to −0.4‰ ($n=76$). $\delta^{18}O_{pc}$ values average −2.6 ± 2.5‰ and range from −6.9 to +4.5‰ (Fig. 4). Both $\delta^{13}C_{pc}$ and $\delta^{18}O_{pc}$ values increase from the early Pliocene to the top of the section at 0.7 Ma; linear regressions of δ values with age yield R^2 values of 0.29 and 0.51 for $\delta^{13}C$ and $\delta^{18}O$, respectively. Isotope data are grouped based on their association with fine or coarse-grained deposits, which indicates the presence of axial or marginal fluvial systems, respectively. Parsing the data in this way shows that $\delta^{18}O_{pc}$ values from fine-grained systems are generally higher than $\delta^{18}O_{pc}$ values of their coarse-grained counterparts ($p=0.0002$), but there is no significant variation in $\delta^{13}C$ values between the marginal and axial floodplain deposits ($p=0.7$) (Figs. 4, 5). However for both the coarse and fine samples there is a positive correlation between $\delta^{13}C$ and $\delta^{18}O$ values; the correlation coefficient, r, is 0.63 and 0.45 for paleosols associated with coarse and fine sediments, respectively.

3.3. Koobi Fora Formation

Pedogenic carbonates were sampled from 105 paleosols in the Koobi Fora Formation from the Moiti through the Okote Members in collection Areas 41, 103, 104, 105, 117, 118, 129, 130, 131, 203, 204 and 261 (Fig. 1). The majority of these samples come from targeted collections of specific stratigraphic intervals associated with the Moiti, Tulu Bor, and KBS tuffs; many of these intervals are the same as those used for systematic faunal sampling (e.g., Behrensmeyer et al., 2004). $\delta^{13}C_{pc}$ and $\delta^{18}O_{pc}$ values were only measured from one nodule for the majority of the Koobi Fora samples.

Pedogenic carbonates sampled for this study within the Koobi Fora Formation yield $\delta^{13}C_{pc}$ values that average −6.7 ± 1.6‰ and range from −10.6 to −2.0‰. $\delta^{18}O_{pc}$ values average −3.1 ± 1.8‰ and range from −7.6 to +1.6‰ ($n=105$). $\delta^{13}C_{pc}$ values from the Koobi Fora Formation increase from the Pliocene through Pleistocene ($R^2=0.25$), but there are no strong trends among the $\delta^{18}O_{pc}$ data from this study alone ($R^2=0.006$), (Fig. 4).

3.4. Time slices

The extensive distribution of tephra throughout the Omo Group deposits enables comparison of pedogenic carbonates from paleosols above and/or below specific tephra throughout the basin, providing a unique view of the landscape before and after deposition of volcanic ashes. Here, $\delta^{13}C_{pc}$ and $\delta^{18}O_{pc}$ values from paleosols associated with the Moiti, Tulu Bor, Lokalalei, Kalochoro and KBS Tuffs are presented. The tephra are used to link the pedogenic carbonate records to one

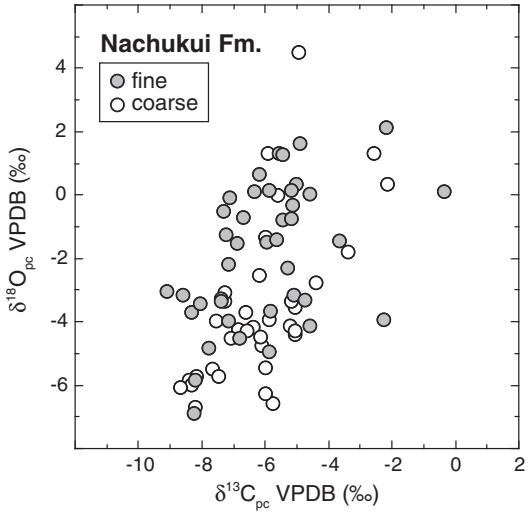

Fig. 5. $\delta^{13}C$ and $\delta^{18}O$ values of pedogenic carbonates from the Nachukui Formation split by association with coarse or fine-grained deposits.

another to form basin-wide snapshots of environmental variation in the soils that directly preceded or followed the deposition of a correlated volcanic ash layer. In some cases (Sections 3.4.3 and 3.4.4) comparisons are made between paleosols within specific sub-members that exist in both the Shungura and Nachukui formations (de Heinzelin, 1983; Harris et al., 1988).

3.4.1. Moiti Tuff (3.97 ± 0.03 Ma)

Just prior to fluvial deposition of the Moiti Tuff, fluvial systems began to dominate the landscape on both the west and east side of the Turkana Basin. Below the Moiti Tuff in the Koobi Fora Formation, fossiliferous sands and fining upward sequences represent the earliest evidence for an axial river system, the ancestral Omo River, which continued deposition above the Moiti Tuff in a similar style (Brown and Feibel, 1991). In the Nachukui Formation, quartz-rich sands and fining upward sequences occur directly below and above the Moiti Tuff. However, unlike the east side of the basin, locally in the Nachukui Formation volcanic cobble conglomerates overlie the first fining upward sequence above the Moiti Tuff and indicate the presence of tributaries draining the basin margin to the west. Paleosols that cap the first fining upward sequence above the Moiti Tuff (3 m above the tuff) were sampled from both the Nachukui and Koobi Fora formations, separated by 60 km (Fig. 6A). $\delta^{13}C_{pc}$ values from these soils in the Nachukui Formation (−8.0 ± 0.6‰, $n = 5$) plot within the range of those from the Koobi Fora Formation (−9.1 ± 1.4‰, $n = 4$) (Fig. 6A), whereas $\delta^{18}O_{pc}$ values in the Nachukui Formation (−5.8 ± 0.8‰, $n = 5$) are higher than $\delta^{18}O_{pc}$ values (−1.4 ± 1.0‰, $n = 4$) from this same level in the Koobi Fora Formation.

3.4.2. Tulu Bor Tuff (3.44 ± .02 Ma)

The depositional context of the Tulu Bor Tuff varies greatly within the Omo–Turkana Basin. In the Nachukui Formation, the Tulu Bor Tuff is preserved in lake-margin, lacustrine diatomites, axial river and tributary river settings, whereas it is associated with large axial river systems and lacustrine diatomites in the Koobi Fora Formation, and associated only with axial river deposits in the Shungura Formation. Paleosol carbonates were sampled directly below and above the Tulu Bor Tuff in the Nachukui and Koobi Fora formations, but not from the Shungura Formation where none of the paleosols were calcareous.

$\delta^{13}C_{pc}$ and $\delta^{18}O_{pc}$ results from different facies beneath the Tulu Bor Tuff are plotted in Fig. 6B for the Nachukui Formation and for Areas 129 and 117 in the Koobi Formation. Paleosols within 5 m of the base of the Tulu Bor Tuff are included in this comparison. $\delta^{13}C_{pc}$ values from the Nachukui Formation plot within the range of $\delta^{13}C_{pc}$ values (−9.1 to −4.8‰) from Koobi Fora Formation paleosols that underlie the Tulu Bor Tuff (Fig. 6B); however the Nachukui Formation $\delta^{18}O_{pc}$ values average −5.4 ± 0.4‰ ($n = 3$) and are lower than $\delta^{18}O_{pc}$ values of most the Koobi Fora samples which average −3.5 ± 1.6‰ ($n = 38$). The difference in $\delta^{18}O_{pc}$ values may be due deposition on the steeper fault margin (Nachukui) versus in the basin axis and ramp margin of the asymmetric half graben (Koobi Fora). In sequences of stacked paleosols sampled beneath the Tulu Bor Tuff in Area 129 of the Koobi Fora Formation there are also discernible changes in both $\delta^{13}C_{pc}$ and $\delta^{18}O_{pc}$ values at particular sites that represent changes in vegetation and water availability in a single location (see samples 129NL-8, 12, 13, 17 in Supplementary Data Table 1).

Paleosols in fining-upward sequences directly above the Tulu Bor Tuff (within 2 m) record local environmental conditions as the

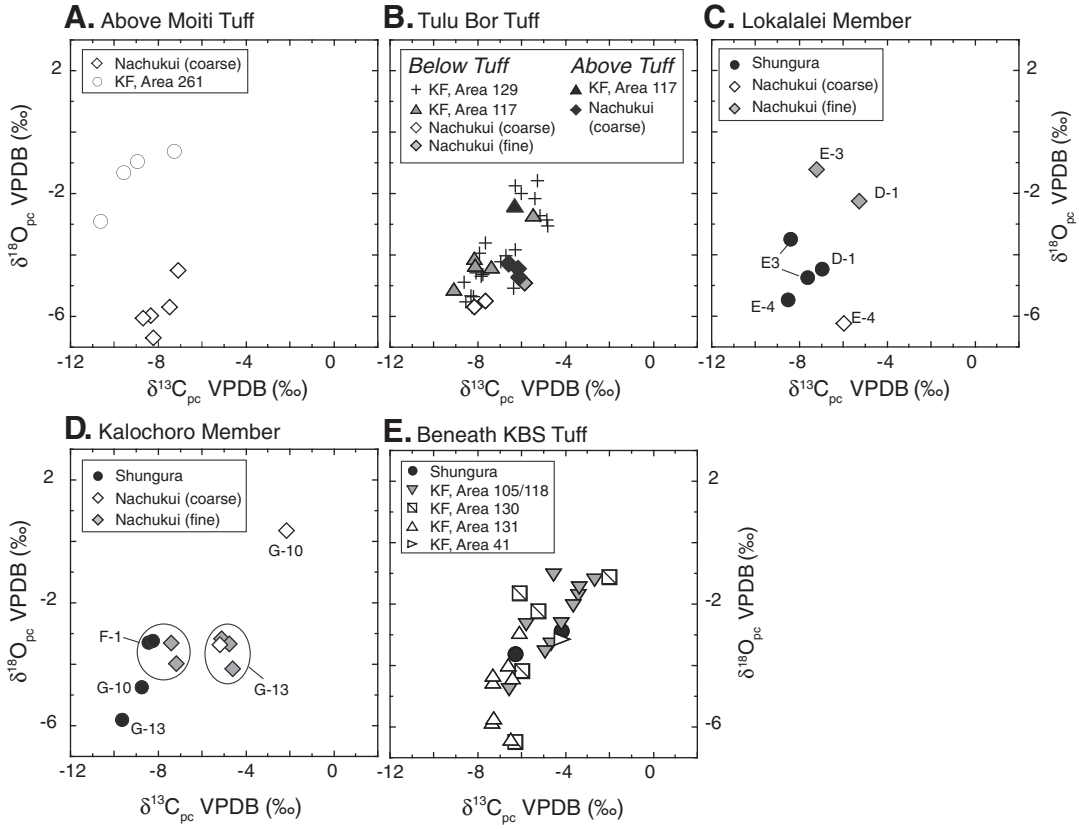

Fig. 6. $\delta^{13}C$ and $\delta^{18}O$ values of pedogenic carbonates from Omo Group paleosols. Subplots are from the following stratigraphic positions, A) directly above the Moiti Tuff, B) within 5 m below the Tulu Bor Tuff and 2 m above the Tulu Bor Tuff, C) levels approximately equivalent to Shungura sub members D-1, E-3, and E-4 in the Lokalalei Member, D) levels approximately equivalent to Shungura sub members F-1, G-10, and G-13 in the Kalochoro Member, and E) within 3 m of the base of the KBS Tuff. Results from paleosols in Nachukui Formation are plotted with open or closed symbols based on their association with fine or coarse-grained sediments, respectively. For the Lokalalei and Kalochoro Members, each data point is annotated with sub member name. Data from the Koobi Fora Formation are plotted separately by collection area.

landscape recovered from deposition of the ash. In the Nachukui Formation, the paleosols sampled directly above the Tulu Bor Tuff are associated with small volcaniclastic tributary systems, whereas coeval paleosols in Area 117 of the Koobi Fora Formation formed on floodplains associated with the axial river system. There are only a few data points from this interval but they indicate similar $\delta^{13}C_{pc}$ values from paleosols in both the Nachukui and Koobi Fora formations, whereas soils from the Nachukui Formation yield $\delta^{18}O_{pc}$ values that are lower than those of the single paleosol sampled in the Koobi Fora Formation from this horizon (Fig. 6B). Isotopic data from paleosols directly above the Tulu Bor Tuff are within the range of $\delta^{13}C$ and $\delta^{18}O$ values from paleosols directly below the tuff (Fig. 6B), indicating that vegetation and hydrological conditions had recovered to their previous state in the first pedogenic interval after deposition of the ash.

3.4.3. Lokalalei Member (2.52–2.33 Ma)

Between 2.52 and 2.33 Ma, many tuffs occur in the Nachukui and Shungura formations. Tuffs D and E in the Shungura Formation correspond to the Lokalalei and Kokiselei Tuffs in the Lokalalei Member of the Nachukui Formation (Harris et al., 1988; Fig. 2). During this time interval, axial river deposits are prevalent in both the Nachukui and Shungura formations, although volcanic pebble conglomerates also outcrop in the Nachukui Formation in the western margin of the basin. Paleosols at three distinct stratigraphic levels between Tuffs D and E (sub members D-1, E-3 and E-4) were sampled in both the Shungura and Nachukui formations ($n=6$) (Fig. 6C). There are no deposits of this age in the Koobi Fora Formation.

The comparison among paleosols in the 2.52–2.33 Ma interval shows that pedogenic carbonates from the Shungura Formation yield lower $\delta^{13}C_{pc}$ values than coeval paleosols from the Nachukui Formation. In two of out three comparisons, pedogenic carbonates from the Shungura Formation yield lower $\delta^{18}O_{pc}$ values than paleosols from the Nachukui Formation. The exception to this occurs at the E-4 level, where the Nachukui paleosol is associated with gravel systems and represents deposition by streams draining the basin margin to the west, not the axial river system coming from the north.

3.4.4. Member F and lower Member G (2.32–2.12 Ma)

In Member F and lower Member G (2.32–2.12 Ma), the ancestral Omo River continues to dominate deposition in the Shungura Formation, while there was deposition of both axial and marginal river sediments in the Nachukui Formation at this time. Sediments are missing from this time interval in the Koobi Fora Formation. Paleosols were sampled from three horizons in the Shungura Formation (sub members F-1, G-10 and G-13) and nearly equivalent levels in the Nachukui Formation.

Carbon isotope results from the Kalochoro Member in the Nachukui Formation show a range in offsets from coeval paleosols in the Shungura Formation. At the F-1 level, $\delta^{13}C_{pc}$ values from the Nachukui Formation are 1‰ higher than $\delta^{13}C_{pc}$ values from the equivalent strata in the Shungura Formation (Fig. 6D). At the levels of G-10 and G-13, $\delta^{13}C_{pc}$ values from paleosols in the Nachukui Formation are 5–7‰ higher than $\delta^{13}C_{pc}$ values from coeval paleosols in the Shungura Formation. $\delta^{18}O_{pc}$ values from the Nachukui Formation are indistinguishable from those in the Shungura Formation at F-1, but higher at levels G-10 and G-13 than their Shungura counterparts.

3.4.5. KBS Tuff (1.868 ± 0.07 Ma)

The KBS tuff is the first basin-wide tephra to appear after the initiation of the major lacustrine interval that began ~2.06 Ma (McDougall and Brown, 2008) and serves as an important marker bed for hominid fossil discoveries, archaeological sites, and basin dynamics (Brown and Feibel, 1991; Isaac, 1997). In the Shungura and Koobi Fora formations, the KBS Tuff was deposited in deltaic sequences after regression of the lake, whereas in the Nachukui Formation it is found primarily in lacustrine and marginal lacustrine deposits (Harris et al., 1988). In the Koobi Fora and Shungura formations, paleosol carbonates were sampled directly below the KBS Tuff and represent the first episodes of soil development as the landscape recovered after the retreat of the Lorenyang Lake. Paleosols associated directly with the KBS Tuff were not sampled from the Nachukui Formation because no appropriate paleosols were identified.

In the Koobi Fora Formation, paleosols within 3 m below the KBS Tuff in Areas 105, 118, 130, 131, and 41 yield average $\delta^{13}C_{pc}$ and $\delta^{18}O_{pc}$ values of -5.4 ± 1.6‰ and -3.4 ± 1.7‰ ($n=24$), respectively (Fig. 6E). There is considerable topography on the basal surface of the KBS Tuff and the paleosols lying directly beneath the tuff cannot be considered to be totally isochronous. In the Shungura Formation pedogenic carbonate from paleosols in two fluvial fining upward sequences <4.5 m below H-2 (the KBS tuff) yield $\delta^{13}C_{pc}$ and $\delta^{18}O_{pc}$ values that average -5.2 ± 1.5‰ and -3.2 ± 0.5‰ ($n=2$). Paleosols within this group show a strong positive correlation between $\delta^{13}C_{pc}$ and $\delta^{18}O_{pc}$ values ($r=0.78$).

4. Discussion

4.1. Environmental variability and change in the Omo–Turkana Basin

These data show that $\delta^{13}C_{pc}$ and $\delta^{18}O_{pc}$ values vary with depositional environment and tectonic setting along the ancestral Omo River drainage as a function of local facies and basin geometry. Our discussion of the data emphasizes three trends: (1) distinctions in $\delta^{13}C_{pc}$ values between axial river floodplain deposits in the Shungura Formation and those from paleosols to the south and downstream (i.e., Nachukui and Koobi Fora formations), (2) the distribution of $\delta^{18}O_{pc}$ values along the ancestral Omo River, and (3) the distribution of $\delta^{18}O_{pc}$ values on floodplains of tributary systems versus those from the floodplains of the axial river system.

$\delta^{13}C_{pc}$ values from the Shungura Formation are lower than $\delta^{13}C_{pc}$ values from coeval paleosols in the Nachukui and Koobi Fora formations, for both comparisons of the different formations (Fig. 4) and of specific time intervals (Fig. 6), for which there are fewer data but greater temporal resolution. The downstream increase in $\delta^{13}C_{pc}$ values along the Omo River is demonstrated in Members D, E, F, and G (Fig. 6C–D). These trends indicate that the floodplain of the ancestral Omo River supported more C_4 grasses and potentially more moisture-stressed C_3 vegetation downstream where the river system was wider, as hypothesized by Brown and Feibel (1991). Although apparent from only several data points at some time intervals, the coherency of these trends suggest that basin position, separating paleosols by ~10^5 m, may be a stronger determinant of $\delta^{13}C_{pc}$ values than more local (10^1–10^4 m) variation associated with differences within and between facies. The $\delta^{13}C_{pc}$ values from the Shungura Formation indicate that C_3-dominated environments were prevalent along the upstream banks of the ancestral Omo River and likely reflect a riparian woodland that was seasonally well-watered. $\delta^{13}C_{pc}$ values from the paleosols in Member H of the Shungura Formation (Fig. 4) are an exception as they plot in the range of $\delta^{13}C_{pc}$ values from coeval deposits downstream in the Koobi Fora Formation. The positive shift in $\delta^{13}C_{pc}$ values in the Shungura Formation from paleosols in Member G (Fig. 4) paleosols signifies a major restructuring of vegetation along the Omo River after regression of the Lorenyang Lake, as suggested previously (Feibel et al., 1991).

The along-axis positive trend in $\delta^{13}C_{pc}$ values is accompanied by a positive trend in $\delta^{18}O_{pc}$ values. Among paleosols that cap fine-grained axial river deposits there is a downstream increase in $\delta^{18}O_{pc}$ values within specific time intervals. For example, among paleosols associated with axial river deposits in the Lokalalei Member, $\delta^{18}O_{pc}$ values in the Nachukui Formation are higher than $\delta^{18}O_{pc}$ values from coeval

paleosols farther upstream in the Shungura Formation (Fig. 6C). This is consistent with the overall correlation of $\delta^{13}C_{pc}$ and $\delta^{18}O_{pc}$ values among all of the paleosols sampled for this study ($r = 0.49$). The downstream increase in $\delta^{13}C_{pc}$ and $\delta^{18}O_{pc}$ values indicate some combination of increased prevalence of C_4 vegetation, decreased soil moisture, increased light stress, decreased soil productivity and differences in the seasonality of pedogenic carbonate precipitation along the ancestral Omo River.

Isolating the effects responsible for these results is difficult, however all of these explanations are consistent with broader floodplains in the Nachukui and Koobi Fora formations that experienced more moisture stress and more turnover of vegetation downstream relative to the upstream river system in the Shungura Formation, where a narrower floodplain and restricted zone of deposition may have facilitated more C_3 vegetation (woody cover), higher soil productivity, less seasonal water stress and decreased soil water evaporation during carbonate precipitation. The explanation for this variation must be reconciled with the existing clumped isotope paleothermometry results that show relative homogeneity in soil temperatures in the Shungura and Nachukui formations (Passey et al., 2010); some combination of shading, ground cover, and moisture kept soils at a similarly high (~35 °C) temperature throughout the Omo–Turkana Basin despite variation in vegetation and depositional mode. A more detailed soil temperature record may help clarify the intra-basin variation in ecology and soil conditions that result in the observed $\delta^{13}C_{pc}$ and $\delta^{18}O_{pc}$ values.

A break in the basin-wide isotopic pattern occurs in paleosols from Members F and G, which show little to no difference between $\delta^{18}O_{pc}$ values in the Shungura and Nachukui formations, while preserving distinctions in $\delta^{13}C_{pc}$ (Fig. 6D). The lack of an oxygen isotope gradient in pedogenic carbonates along the ancestral Omo River indicates smaller differences in soil moisture along the axial river floodplain, which may be related to the changes in basin dynamics that resulted in higher deposition rates.

The third major observation is that $\delta^{18}O_{pc}$ values from coarse-grained marginal deposits are lower than $\delta^{18}O_{pc}$ values from paleosols associated with fine-grained sediments. This trend is exhibited in the plot of $\delta^{18}O_{pc}$ values from Nachukui Formation paleosols distinguished by their association with fine or coarse-grained sediment (Fig. 5). The same trend is apparent among the paleosol isochrons associated with the Moiti Tuff, the Tulu Bor Tuff and in the Lokalalei Member, where $\delta^{18}O_{pc}$ values from paleosols associated with coarse-grained and marginal fluvial deposits in the Nachukui Formation are up to 5‰ lower than $\delta^{18}O_{pc}$ values from paleosols that are associated with fine-grained sediments and developed on floodplains of the axial river system (Fig. 6A–D). The 5‰ difference between $\delta^{18}O_{pc}$ values on the floodplains of marginal and axial river systems may be due to: (1) basin margin soils were 25 °C warmer (assuming −0.2‰/°C equilibrium fractionation reported by Kim and O'Neil, 1997), (2) $\delta^{18}O$ values of rainfall west of the basin were lower than $\delta^{18}O$ values of precipitation supplying soil water to the axis of the basin, or (3) there was less evaporation in the marginal river overbank deposits than on the floodplain of the axial river system. The first explanation can be dismissed because a 25 °C difference in soil temperature is unlikely in the small distances (<10 km) over which some of these differences in $\delta^{18}O_{pc}$ values are observed; such a temperature range is more than twice that observed for the pedogenic carbonates from the Nachukui Formation (Passey et al., 2010). Explanations involving differences in water source and evaporation are more plausible and may be a function of the seasonality of carbonate precipitation in soils on the basin margins versus those in the basin axis. If there was seasonal variation in $\delta^{18}O$ values of rainfall during the Pliocene and Pleistocene, as there is today in East Africa (Rozanski et al., 1996), lower $\delta^{18}O_{pc}$ values from coarse-grained marginal deposits may reflect carbonate precipitation during seasons when rainfall $\delta^{18}O$ values were low, during seasons where rainfall amount was higher than normal, or when moisture came from a distinct source. Alternatively, the low $\delta^{18}O_{pc}$ values associated with coarse-grained facies may reflect carbonate formation from soil water that did not experience considerable evaporation, due to a shorter residence time of soil water, more humid conditions in these basin margin soils, or differences in water demands of vegetation. We cannot tease apart the latter two explanations with the present data but low rainfall $\delta^{18}O$ values and reduced soil water evaporation may have worked in concert to produce $\delta^{18}O_{pc}$ from basin-margin paleosols that were lower than their counterparts from the basin axis.

The isotopic results from the basin-wide sampling of short stratigraphic intervals demonstrate that the soils in the Omo–Turkana Basin hosted a diversity of vegetation communities and hydrologic environments, reflecting contrasts in water availability, slope, and drainage across short distances. These results highlight the importance of considering depositional setting when interpreting isotopic records of pedogenic of carbonate in the context of regional or global climate trends.

4.2. Comparison with other paleosol records from Turkana

This study expands the existing dataset of pedogenic carbonate isotope ratios from the Omo Group deposits. The Koobi Fora carbon isotope record presented here complements records from Cerling et al. (1988) and Quinn et al. (2007). Results from detailed sampling above and below the Tulu Bor Tuff expand the range of $\delta^{13}C_{pc}$ values for this time interval. Higher in the stratigraphic section, intensive sampling of paleosols below the KBS tuff demonstrates high $\delta^{13}C_{pc}$ values (−2‰) at Koobi Fora at 1.88 Ma, prior to the shift to C_4 environments at 1.8 Ma that was recognized by Cerling et al. (1988) and supported through observations by Quinn et al. (2007).

The $\delta^{13}C_{pc}$ record from the Nachukui Formation generally corroborates the trends observed by Wynn (2004), with some notable exceptions. The three intervals of rapid increase in mean $\delta^{13}C_{pc}$ values 3.58 Ma, 2.52 Ma and 1.8 Ma in the Nachukui Formation recognized by Wynn (2004) become less apparent with the addition of data from this study (Fig. 4). The prospect that samples were collected in different locations likely explains differences in the records and is consistent with lateral variability observed elsewhere.

The Shungura record provides a new window into environments of the lower Omo River Valley during the Pliocene and shows that vegetation and hydrological conditions adjacent to the Omo River in the Shungura Formation were different than farther south in the basin. $\delta^{13}C$ values of paleosol carbonates suggest that trees and shrubs flanked the paleo-Omo River, except for the latest portions of the record sampled when paleosol carbonate $\delta^{13}C$ values increase to −4.5‰ (Fig. 4). Although this increase may partially reflect the effects of increased aridity on the existing C_3 biomass, we view the increased abundance of C_4 plants in the soils flanking the Omo River as primarily responsible for the increase in $\delta^{13}C_{pc}$ values because it is difficult to explain the high $\delta^{13}C_{pc}$ values from 1.88 to 1.18 Ma (Figs. 4, 7, Section 3.2) in the Shungura Formation without the presence of C_4 vegetation.

Of the isotopic records from the Omo Group paleosols, oxygen isotope data are discussed by Cerling et al. (1988) and only briefly mentioned by Wynn (2004). From the $\delta^{18}O_{pc}$ data, these studies conclude that there are varying degrees of evaporative enrichment of ^{18}O in soil waters and that rainfall $\delta^{18}O$ values must have been more negative in the past. Oxygen isotope records from this study support these two conclusions, and provide additional perspective on how $\delta^{18}O_{pc}$ values vary within the Omo–Turkana Basin, in terms of (1) a downstream increase in $\delta^{18}O_{pc}$ values along the floodplain of the Omo River, and (2) lower $\delta^{18}O_{pc}$ values from basin margin deposits relative to $\delta^{18}O_{pc}$ values associated with axial river deposits. The basin-wide increase in soil water $\delta^{18}O$ values between 2.0 and 1.8 Ma was likely a response to a shift in regional climate that increased $\delta^{18}O$ values of

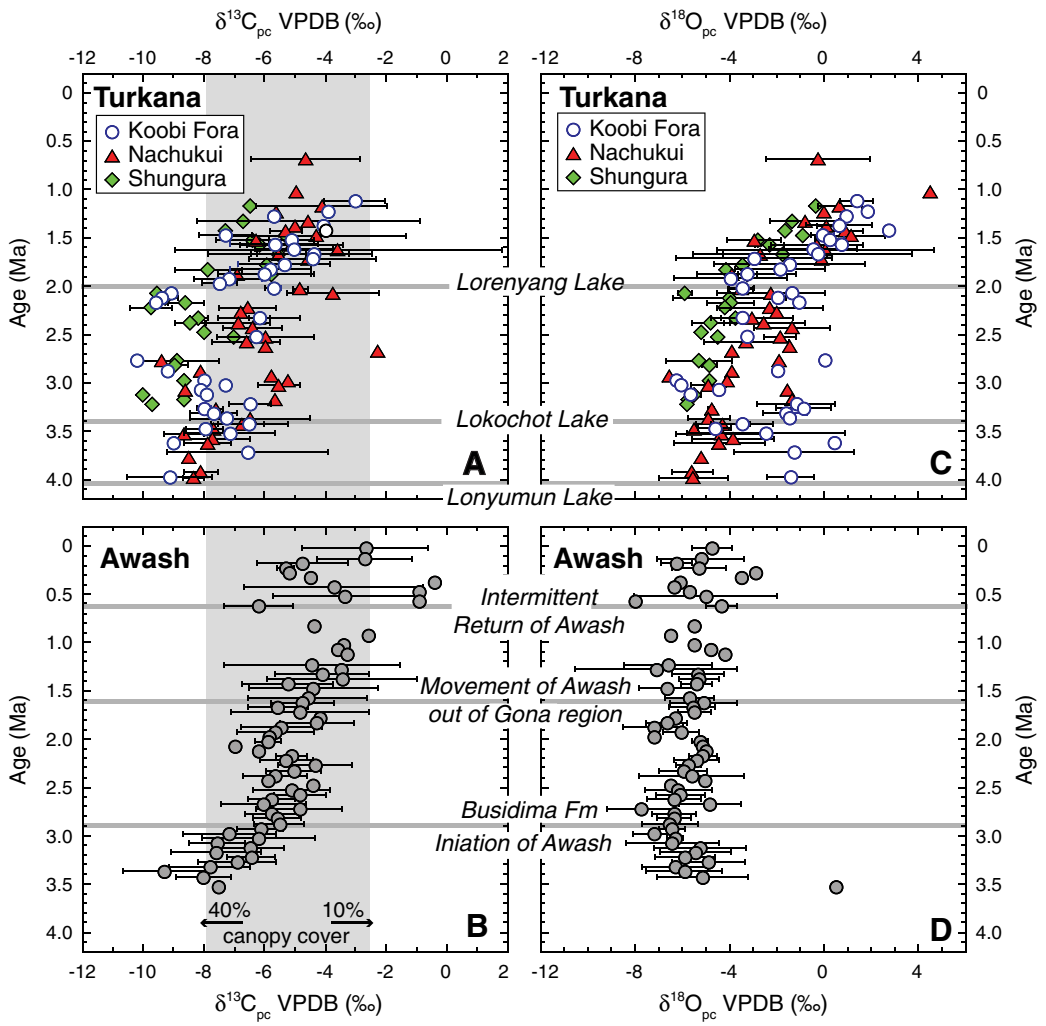

Fig. 7. $\delta^{13}C$ (a, b) and $\delta^{18}O$ (c, d) values of pedogenic carbonates from the Omo–Turkana and Awash Basins binned by 50 kyr time intervals. The Omo Group data include the following formations: Shungura (this study), Koobi Fora (this study; Cerling et al., 1988; Quinn et al., 2007, $\delta^{13}C$ only), Nachukui (this study and Wynn, 2004). Data for the Awash Basin are from published records for the last 4.0 Ma from the Awash Basin (Levin et al., 2004; Quade et al., 2004; Wynn et al., 2006; Aronson et al., 2008; Passey et al., 2010; Quade and Levin, in press). Ages of samples are interpolated from the stratigraphic distance between dated horizons. Error bars represent 1σ error on the mean; where there is only 1 sample for a 50 kyr bin, isotopic values are reported without error bars. The timing of major depositional events and transitions in each basin is marked by gray horizontal bars based on Quade et al. (2008) and Brown and Feibel (1991). Gray shading behind (a) and (b) indicates the range of $\delta^{13}C_{pc}$ values expected for soils where there is 40–10% woody canopy cover as calculated by Cerling et al. (2010), assuming that the enrichment between soil organic matter and pedogenic carbonate $\delta^{13}C$ values is 16‰. Smaller organic matter to carbonate $\delta^{13}C$ offsets would shift this shaded zone towards more negative $\delta^{13}C_{pc}$ values.

rainfall reaching the Omo–Turkana Basin and decreased rainfall amounts. Although such a shift in soil water $\delta^{18}O$ may have been triggered by ecological factors alone, a shift in climate patterns was likely a factor in determining the trend in $\delta^{18}O_{pc}$ values, as discussed below.

4.3. Omo–Turkana versus Awash

The existence of a Plio-Pleistocene pedogenic carbonate isotope record from the Awash Basin in Ethiopia, 800 km northeast of Lake Turkana, makes it possible to compare the Omo Group pedogenic carbonate isotope record to a contemporaneous record in East Africa (Fig. 1). Like the Omo–Turkana Basin, the Awash Basin is host to abundant material and fossil evidence for human evolution (e.g., Johanson et al., 1982; Clark et al., 1994; Kimbel et al., 1994; Semaw et al., 1997; Alemseged et al., 2006; Simpson et al., 2008; White et al., 2009). Fossil rich sediments in the Awash Basin are exposed by incision of the Awash River today, which flows to the northeast from the central Ethiopian Highlands (Quade et al., 2004, 2008) (Fig. 1). Several paleosol isotopic records from the lower Awash Basin document environmental change since 4.0 Ma and provide a useful comparison for the isotopic record from the Omo Group (Levin et al., 2004; Quade et al., 2004; Wynn et al., 2006; Aronson et al., 2008). Despite the brief but significant lacustrine deposits in the Hadar Formation >3.3–3.24 Ma, Pliocene and Pleistocene sediments since 4.0 Ma in the lower Awash Basin are dominated by fluvial deposition (Kimbel et al., 1996; Campisano and Feibel, 2008; Quade et al., 2008; Wynn et al., 2008). The introduction of large cobble conglomerates ~2.9–2.7 Ma, considered to be deposits of the ancestral Awash River, created a significant unconformity in the lower Awash Basin and marks the distinction between the Hadar Formation below and the Busidima Formation above (Quade et al., 2004, 2008).

The paleosol isotope records from the Hadar and Busidima formations and the Omo Group deposits offer two distinct, semi-continuous records of river systems that drained the Ethiopian highlands. Here, the records are briefly compared, first by focusing on the time interval between 2.9 and 2.0 Ma when there is strong evidence for axial river deposition in both the Omo–Turkana and Awash basins, and then by comparing temporal trends in $\delta^{13}C_{pc}$ and $\delta^{18}O_{pc}$ values over the full extent of the records from both regions.

Among paleosols sampled between 2.9 and 2.0 Ma, $\delta^{13}C_{pc}$ values from the Busidima Formation ($n=113$) are higher on average than $\delta^{13}C_{pc}$ values in the Nachukui Formation ($n=50$, $p=0.0001$) and in the Shungura Formation ($n=32$, <0.0001) (Fig. 7). In contrast, average $\delta^{18}O_{pc}$ values from the Busidima Formation are significantly lower than $\delta^{18}O_{pc}$ values from both the Shungura and Nachukui formations in this time interval ($p<0.0001$), although there is overlap in the range of $\delta^{18}O_{pc}$ values from the Shungura and Busidima formations (Fig. 7). Paleosols from the Koobi Fora Formation are not included in this comparison because they are poorly represented between 2.9 and 2.0 Ma.

The $\delta^{13}C_{pc}$ results from the Busidima, Nachukui and Shungura formations suggest that the floodplains of the ancestral Awash River supported more C_4 vegetation than the floodplains of the ancestral Omo River between 2.9 and 2.0 Ma. An alternate explanation of higher $\delta^{13}C_{pc}$ values in the Awash Basin could include higher aridity and light stress that increased the $\delta^{13}C$ values of C_3 plants in the Awash Basin, or lower soil productivity resulting in higher $\delta^{13}C$ values of soil CO_2 in soils with similar proportions of C_4 plants (see discussion in Breecker et al., 2009). However, we view the relative proportion of C_4 plant abundance as the clearest explanation for difference in $\delta^{13}C_{pc}$ values because $\delta^{18}O_{pc}$ values from the Awash Basin are lower in both range and absolute value relative to those from the Omo–Turkana Basin, which is not consistent with the alternate explanations for higher $\delta^{13}C_{pc}$ values in the Awash Basin.

Despite differences between the basins, there are clear increases in $\delta^{13}C_{pc}$ values throughout the Pliocene and Pleistocene in both the Awash and Omo–Turkana Basins. In both basins, these increases are associated with facies changes. The most significant shift in $\delta^{13}C_{pc}$ values in the lower Awash Basin occurs at the transition between the Hadar and Busidima formations (2.9–2.7 Ma) with the marked increase of cobble conglomerates into the system signifying a major shift in depositional mode (Quade et al., 2004). The largest basin-wide shift in $\delta^{13}C$ values in the Omo Group occurs after the regression of Lake Lorenyang, ~2.0 Ma, which signals a major topographic and hydrological reorganization of the Omo–Turkana Basin (Bruhn et al., 2011).

The oxygen isotope record indicates similarities and differences in the hydrological conditions in the Awash and Omo–Turkana Basins. After 2.0 Ma, there is less overlap in $\delta^{18}O_{pc}$ values between these two basins. A shift to more positive $\delta^{18}O_{pc}$ values after 2.0 Ma in the Omo Group is not accompanied by similar increase in $\delta^{18}O$ values in the Busidima Formation. While the offsets in $\delta^{18}O_{pc}$ values between the basins and the shift in $\delta^{18}O_{pc}$ values within the Omo–Turkana Basin can be viewed in terms of variation in soil water evaporation as a function of soil hydrology, vegetation and local aridity, it is critical to consider the effects of the isotopic composition of rainfall on the $\delta^{18}O_{pc}$ record.

$\delta^{18}O_{pc}$ records from both basins indicate that the ^{18}O composition of meteoric waters must have been lower in the past. Minimum $\delta^{18}O_{pc}$ values make the best estimates for meteoric water $\delta^{18}O$ ($\delta^{18}O_{mw}$) values because they represent carbonates that formed from waters that experienced the least amount of evaporation. As reviewed in Section 1.2.2, estimates of soil water values are made from $\delta^{18}O_{pc}$ values, temperature of carbonate formation, and temperature dependent calcite–water fractionation relationships. Clumped isotope paleothermometry of pedogenic carbonates from the Shungura and Nachukui formations from Passey et al. (2010) give us the best estimates of soil temperatures during pedogenic carbonate formation in East Africa during the Pliocene and Pleistocene. Assuming soil temperatures of ~35 °C and fractionation relationships in Kim and O'Neil (1997), and minimum $\delta^{18}O_{pc}$ values, then $\delta^{18}O$ values of rainfall reaching these soils would be less than −4.0‰ (VSMOW) in both basins 2.9–2.0 Ma. Today, $\delta^{18}O_{mw}$ values average −2‰ and −3‰ (VSMOW) for the Awash and Omo–Turkana regions, respectively (Levin et al., 2009). The shift towards more positive $\delta^{18}O_{pc}$ values in the Omo Group after 2.0 Ma, indicates an increase in $\delta^{18}O_{mw}$ values, an increase in soil water evaporation, or a combination of the two. Both of these explanations could reflect the decreased intensity of the Indian Ocean monsoon and less moisture transport to the Omo–Turkana Basin after 2.0 Ma, as has been previously suggested (e.g., deMenocal, 2004; Sepulchre et al., 2006). In contrast, $\delta^{18}O_{pc}$ values in the lower Awash Basin indicate that carbonates continued to form from ^{18}O-depleted waters throughout the Pleistocene and that climate and soil conditions were steady during soil-forming episodes. The Awash $\delta^{18}O_{pc}$ record indicates that there must be some difference between today's climate conditions and those that affected pedogenic intervals in the Pliocene ad Pleistocene; calculated soil water $\delta^{18}O$ values in the Pliocene and Pleistocene are too low to have formed from precipitation with modern $\delta^{18}O_{mw}$ values (Hailemichael et al., 2002; Levin et al., 2004; Aronson et al., 2008). Greater intensity of the southeasterly monsoon during pedogenic intervals could be responsible for this discrepancy as it would result in lower $\delta^{18}O_{mw}$ values in the Awash Basin if the region received the majority of its rainfall from Indian Ocean moisture that traveled across Somalia and Kenya and not from recycled continental moisture as it does today (Levin et al., 2009). If this is the case, the paleosol record in the Awash Basin may be buffered from regional trends in aridity during the Pliocene and Pleistocene, as it may only document climatic intervals when the Indian Monsoon was intense. In contrast, paleosols in the Omo–Turkana Basin record a step-wise shift in hydrology that reflects regional trends towards decreased monsoon intensity and higher aridity after 2.0 Ma.

4.4. Increased abundance of C_4 grasses in floodplain environments

$\delta^{13}C_{pc}$ records from Omo–Turkana and Awash are the most complete temporal record of isotopic variation within paleosol carbonates from East Africa during the Pliocene and Pleistocene. These records provide perspective on the ecology of axial rivers systems and their tributaries in the Omo–Turkana and Awash Basins during critical time periods in human evolution and global climate change. As shown from previous studies, records from both basins demonstrate the increased presence of C_4 vegetation in floodplain paleosols through the Pliocene and Pleistocene (Cerling et al., 1988; Wynn, 2004; Levin et al., 2004; Aronson et al., 2008). Increased sampling of the Omo–Turkana Basin demonstrates that variability in the $\delta^{13}C_{pc}$ record can be a function of depositional context, i.e., within a fluvial system and a rift setting, as shown previously on smaller scales (Levin et al., 2004; Behrensmeyer et al., 2007; Quinn et al., 2007; Sikes and Ashley, 2007). The low $\delta^{13}C_{pc}$ values from the Shungura Formation prior to 2.0 Ma clearly show that C_3-dominated environments can be documented in Plio-Pleistocene East African rift sediments, when present. The Shungura record stands in contrast to coeval soils in the Nachukui and Koobi Fora formations where there was a mix of C_3 and C_4 vegetation, providing clear evidence of environmental differences within the Omo–Turkana Basin over distances of 10^1–10^2 km. The updated $\delta^{13}C_{pc}$ record indicates that there is only one basin-wide transition ~2.0–1.8 Ma, after the retreat of Lake Lorenyang, when there is a shift towards more C_4 vegetation and potentially drier conditions in every depositional setting (Figs. 4, 7). The $\delta^{13}C_{pc}$ data support sedimentological, faunal and palynological indications that environments in the Omo–Turkana Basin were fundamentally changed after the major reorganization of basin geography that resulted in this lacustrine interval (Bonnefille, 1983; Brown and Feibel, 1988; Feibel et al., 1991; Bobe and Behrensmeyer, 2004; Bruhn et al., 2011). The distinct shift towards more C_4 vegetation and less woody cover in floodplain environments after 2.0 Ma is likely a combined effect of both local geographic changes, ecological shifts, and regional climate trends towards increased aridity after 1.8 Ma (deMenocal, 2004), whereas prior to 2.0 Ma, floodplain environments in the Shungura Formation seemed

buffered from regional climate perturbations. The coincidence of regional climate trends and ecological change may reflect the role of geography in affecting the sensitivity of specific environments to larger-scale climate shifts.

5. Conclusions

Fluvial sediments from the Omo–Turkana Basin provide a unique opportunity to characterize terrestrial environmental change regionally in the Pliocene and Pleistocene. Detailed sampling of Omo Group paleosols in three different regions of the basin shows that the distribution of vegetation and water stress is a function of depositional setting. There are clear isotopic indications of a wooded zone in soils associated with the upper reaches of the ancestral Omo River when C_4 grasses were prevalent downstream, where the river system occupied a broader portion of the rift basin. The transition to C_4-dominated soil forming environments after 2.0 Ma in the Omo Group sediments coincided with the draining of Lake Lorenyang, an event that altered the vegetation and water balance across a diverse set of depositional environments and tectonic settings. Recognition of this basin wide event is critical when interpreting the implications of the isotopic record of pedogenic carbonates from the region.

The compilation of paleosol carbonate isotope data from this study makes it clear that terrestrial environments in East Africa did not respond uniformly to climate change in the Pliocene and Pleistocene. Interbasinal comparisons indicate that there was a greater proportion of C_4 vegetation on the floodplains of the lower Awash Basin than in the Omo–Turkana Basin 2.9–2.0 Ma. After 2.0 Ma, the prevalence of C_4 vegetation on floodplains in the two basins is comparable but differences in $\delta^{18}O_{pc}$ values between the basins suggest that they were sensitive to different climatic parameters.

Amidst these differences, paleosol records from these two basins reveal a common ecological trend: the steady increase of C_4 plants in floodplain environments since 4 Ma. This increase occurred well after some African mammalian lineages adapted to C_4-dominated diets in the late Miocene. Although C_4 plants had been significant parts of East African landscapes, this later shift in $\delta^{13}C_{pc}$ values documents the prevalence of open environments, even along axial rivers where trees and shrubs would be most likely.

Supplementary materials related to this article can be found online at doi:10.1016/j.palaeo.2011.04.026.

Acknowledgments

We thank Patrick Gathogo, Getachew Eshete, Tesfaye Kidane, and Kevin Uno for their help in the field, and Kevin Uno and David Dettman for help in the laboratory. Collection of samples from the Koobi Fora Formation was in collaboration with David Braun, Christopher Campisano and Jack Harris. We thank Jonathan Wynn and Rhonda Quinn for providing their published data in tabulated form. The National Museums of Kenya were critical for the export of samples. We thank Jay Quade for discussions that sparked many of the ideas and data presented here. We are also grateful to David Fox and an anonymous reviewer for their constructive comments that improved the manuscript. This research was funded with grants from the International Association of Sedimentologists, the Leakey Foundation, and the National Science Foundation (BCS0621542).

References

Ahmad, N., 1983. Vertisols. In: Wilding, L.P., Smeck, N.E., Hall, G.F. (Eds.), Pedogenesis and Soil Taxonomy. Elsevier, New York, pp. 91–123.
Alemseged, Z., Spoor, F., Kimbel, W.H., Bobe, R., Geraads, D., Reed, D., Wynn, J.G., 2006. A juvenile early hominin skeleton from Dikika, Ethiopia. Nature 443, 296–301.
Amundson, R., Chadwick, O., Kendall, C., Wang, Y., Deniro, M., 1996. Isotopic evidence for shifts in atmospheric circulation patterns during the late Quaternary in mid-North America. Geology 24, 23–26.
Aronson, J.L., Hailemichael, M., Savin, S.M., 2008. Hominid environments at Hadar from paleosol studies in a framework of Ethiopian climate change. Journal of Human Evolution 55, 532–550.
Ashley, G.M., 2007. Orbital rhythms, monsoons, and playa lake response, Olduvai Basin, equatorial East Africa (ca. 1.85–1.74 Ma). Geology 35, 1091–1094.
Barnes, C.J., Turner, J.V., 1998. Isotopic exchange in soil water. In: Kendall, C., McDonnell, J.J. (Eds.), Isotope Tracers in Catchment Hydrology. Elsevier, Amsterdam, pp. 137–163.
Behrensmeyer, A.K., Bobe, R., Campisano, C.J., Levin, N., 2004. High resolution taphonomy and paleoecology of the Plio-Pleistocene Koobi Fora Formation, northern Kenya, with comparisons to the Hadar Formation, Ethiopia. Journal of Vertebrate Paleontology 24 (Supplement to #3), 38A.
Behrensmeyer, A.K., Quade, J., Cerling, T.E., Kappelman, J., Khan, I.A., Copeland, P., Roe, L., Hicks, J., Stubblefield, P., Willis, B.J., Latorre, C., 2007. The structure and rate of late Miocene expansion of C_4 plants: Evidence from lateral variation in stable isotopes in paleosols of the Siwalik Group, northern Pakistan. Geological Society of America Bulletin 119, 1486–1505.
Bobe, R., Behrensmeyer, A.K., 2004. The expansion of grassland ecosystems in Africa in relation to mammalian evolution and the origin of the genus *Homo*. Palaeogeography, Palaeoclimatology, Palaeoecology 207, 399–420.
Bonnefille, R., 1983. Evidence for a cooler and drier climate in the Ethiopian uplands towards 2.5 Myr ago. Nature 303, 487–491.
Breecker, D.O., Sharp, Z.D., McFadden, L.D., 2009. Seasonal bias in the formation and stable isotopic composition of pedogenic carbonate in modern soils from central New Mexico, USA. Geological Society of America Bulletin 121, 630–640.
Brown, F.H., Feibel, C.S., 1988. "Robust" hominids and Plio-Pleistocene paleogeography of the Turkana Basin, Kenya and Ethiopia. In: Grine, F.E. (Ed.), Evolutionary history of the "Robust" Australopithecines. Aldine de Gruyter, New York, pp. 325–341.
Brown, F.H., Feibel, C.S., 1991. Stratigraphy, depositional environments, and palaeogeography of the Koobi Fora Formation. In: Harris, J.M. (Ed.), Koobi Fora Research Project. : The Fossil Ungulates: Geology, Fossil Artiodactyls, and Palaeoenvironments, Vol. 3. Clarendon Press, Oxford, pp. 1–30.
Brown, F., Harris, J., Leakey, R., Walker, A., 1985. Early *Homo erectus* skeleton from west Lake Turkana, Kenya. Nature 316, 788–792.
Brown, F.H., Sarna-Wojcicki, A.M., Meyer, C.E., Haileab, B., 1992. Correlation of Pliocene and Pleistocene tephra layers between the Turkana Basin of East Africa and the Gulf of Aden. Quaternary International 13 (14), 55–67.
Brown, F.H., Haileab, B., McDougall, I., 2006. Sequence of tuffs between the KBS Tuff and the Chari Tuff in the Turkana Basin, Kenya and Ethiopia. Journal Geological Society London 163, 185–204.
Bruhn, R.L., Brown, F.H., Gathogo, P.N., Haileab, B., 2011. Pliocene volcano-tectonics and paleogeography of the Turkana Basin, Kenya and Ethiopia. Journal of African Earth Sciences 59, 295–312.
Campisano, C.J., Feibel, C.S., 2008. Depositional environments and stratigraphic summary of the Pliocene Hadar Formation at Hadar, Afar Depression, Ethiopia. In: Quade, J., Wynn, J.G. (Eds.), The Geology of Early Humans in the Horn of Africa: Geological Society of America Special Paper, 446, pp. 179–201.
Cande, S.C., Kent, D.V., 1995. Revised calibration of the geomagnetic polarity timescale for the Late Cretaceous and Cenozoic. Journal of Geophysical Research 100, 6093–6095.
Cane, M.A., Molnar, P., 2001. Closing of the Indonesian seaway as a precursor to east African aridification around 3–4 million years ago. Nature 411, 157–162.
Cerling, T.E., 1986. A mass-balance approach to basin sedimentation: constraints on the recent history of the Turkana Basin. Palaeogeography, Palaeoclimatology, Palaeoecology 54, 63–86.
Cerling, T.E., 1992. Development of grasslands and savannas in East Africa during the Neogene. Palaeogeography, Palaeoclimatology, Palaeoecology 97, 241–247.
Cerling, T.E., 1999. Stable carbon isotopes in palaeosol carbonates. In: Thiry, M., Simon-Coincon, R. (Eds.), Palaeoweathering, palaeosurfaces and related continental deposits: Special Publications of the International Association of Sedimentology, pp. 43–60.
Cerling, T.E., Quade, J., 1993. Stable carbon and oxygen isotopes in soil carbonates. In: Swart, P.K., Lohmann, K.C., McKenzie, J., Savin, S. (Eds.), Climate change in continental isotopic records: Geophysical Monograph. American Geophysical Union, pp. 217–231.
Cerling, T.E., Bowman, J.R., O'Neil, J.R., 1988. An isotopic study of a fluvial-lacustrine sequence: the Plio-Pleistocene Koobi Fora sequence, East Africa. Palaeogeography, Palaeoclimatology, Palaeoecology 63, 335–356.
Cerling, T.E., Solomon, D.K., Quade, J., Bowman, J.R., 1991. On the isotopic composition of carbon in soil carbon dioxide. Geochimica et Cosmochimica Acta 55, 3403–3405.
Cerling, T.E., Harris, J.M., Passey, B.H., 2003. Diets of East African Bovidae based on stable isotope analysis. Journal of Mammalogy 84, 456–470.
Cerling, T.E., Levin, N.E., Quade, J., Wynn, J.G., Fox, D.L., Kingston, J.D., Klein, R.G., Brown, F.H., 2010. Comment on the Paleoenvironment of *Ardipithecus ramidus*. Science 328, 1105-d.
Chaisson, W.P., 2000. Pliocene development of the east-west hydrographic gradient in the equatorial Pacific. Paleoceanography 15, 497–505.
Clark, J.D., de Heinzelin, J., Schick, K.D., Hart, W.K., White, T.D., WoldeGabriel, G., Walter, R.C., Suwa, G., Asfaw, B., Vrba, E., Haile-Selassie, Y., 1994. African *Homo erectus*: old radiometric ages and young Oldowan assemblages in the Middle Awash Valley, Ethiopia. Science 264, 1907–1910.
Craig, H., Gordon, L.I., 1965. Deuterium and oxygen-18 variations in the ocean and the marine atmosphere. In: Tongiorgi, E. (Ed.), Stable isotopes in oceanographic studies and paleotemperatures. V. Lischi, Spoleto, Italy, pp. 9–130.
Dansgaard, W., 1964. Stable isotopes in precipitation. Tellus 16, 436–468.
Davidson, G.R., 1995. The stable isotopic composition and measurement of carbon in soil CO_2. Geochimica et Cosmochimica Acta 59, 2485–2489.

de Heinzelin, J., 1983. The Omo Group: Archives of the International Omo Research Expedition. Sciences Geologiques No. 85: Musee Royal de L'Afrique Centrale, serie in 8°, Tervuren.
Deino, A.L., Kingston, J.D., Glen, J.M., Edgar, R.K., Hill, A., 2006. Precessional forcing of lacustrine sedimentation in the late Cenozoic Chemeron Basin, Central Kenya Rift, and calibration of the Gauss/Matuyama boundary. Earth and Planetary Science Letters 247, 41–60.
deMenocal, P.B., 2004. African climate change and faunal evolution during the Pliocene–Pleistocene. Earth and Planetary Science Letters 220, 3–24.
East African Meteorological Department, 1975. Climatological Statistics for East Africa. East African Meteorological Department, Nairobi, Kenya.
Farquhar, G.D., Ehleringer, J.R., Hubick, K.T., 1989. Carbon isotope discrimination and photosynthesis. Annual Review of Plant Physiology 40, 503–537.
Feakins, S.J., deMenocal, P.B., Eglinton, T.I., 2005. Biomarker records of late Neogene changes in northeast African vegetation. Geology 33, 977–980.
Feakins, S.J., Eglinton, T.I., deMenocal, P.B., 2007. A comparison of biomarker records of northeast African vegetation from lacustrine and marine sediments (ca. 3.4 Ma). Organic Geochemistry 38, 1607–1624.
Feibel, C.S., 1988. Paleoenvironments of the Koobi Fora Formation, Turkana Basin, Northern Kenya. Ph.D. Thesis, University of Utah, Salt Lake City, 330 pp.
Feibel, C.S., Brown, F.H., McDougall, I., 1989. Stratigraphic context of fossil hominids from the Omo Group deposits: northern Turkana Basin, Kenya and Ethiopia. American Journal of Physical Anthropology 78, 595–622.
Feibel, C.S., Harris, J.M., Brown, F.H., 1991. Palaeoenvironmental context for the late Neogene of the Turkana Basin. In: Harris, J.M. (Ed.), Koobi Fora Research Project. : The Fossil Ungulates: Geology, Fossil Artiodactyls, and Palaeoenvironments Koobi Fora Research Project, Vol. 3. Clarendon Press, Oxford, pp. 321–370.
Francey, R.J., et al., 1999. A 1000-year high precision record of $\delta^{13}C$ in atmospheric CO_2. Tellus 51B, 170–193.
Gani, N.D., Gani, M.R., Abdelsalam, M.G., 2007. Blue Nile incision on the Ethiopian Plateau: pulsed plateau growth, Pliocene uplift, and hominin evolution. GSA Today 17, 4–11.
Haesaerts, P., Stoops, G., van Vliet-Lanoe, B., 1983. Data on sediments and fossil soils. In: de Heinzelin, J. (Ed.), The Omo Group: Archives of the International Omo Research Expedition. Musee Royal de L'Afrique Centrale, Tervuren, pp. 149–185.
Hailemichael, M., Aronson, J.L., Savin, S., Tevesz, M.J.S., Carter, J.G., 2002. $\delta^{18}O$ in mollusk shells from Pliocene Lake Hadar and modern Ethiopian lakes: implications for history of the Ethiopian monsoon. Palaeogeography, Palaeoclimatology, Palaeoecology 186, 81–99.
Harris, J.M., Brown, F.H., Leakey, M.G., 1988. Stratigraphy and paleontology of Pliocene and Pleistocene localities west of Lake Turkana, Kenya. Contributions in Science, Los Angeles County Museum of Natural History, 399, pp. 1–128.
Haug, G.H., Hughen, K.A., Sigman, D.M., Peterson, L.C., Röhl, U., 2001. Southward migration of the Intertropical Convergence Zone through the Holocene. Science 293, 1304–1308.
Hillaire-Marcel, C., Taieb, M., Tiercelin, J.J., Page, N., 1982. A 1.2-Myr record of isotopic changes in a late Pliocene Rift Lake, Ethiopia. Nature 296, 640–642.
Howell, F.C., Haesaerts, P., de Heinzelin, J., 1987. Depositional environments, archeological occurrences and hominids from Members E and F of the Shungura Formation (Omo Basin, Ethiopia). Journal of Human Evolution 16, 665–700.
Hsieh, J.C.C., Chadwick, O.A., Kelly, E.F., Savin, S.M., 1998. Oxygen isotopic composition of soil water: quantifying evaporation and transpiration. Geoderma 82, 269–293.
Imbrie, J., Boyle, E.A., Clemens, S.C., Duffy, A., Howard, W.R., Kukla, G., Kutzbach, J., Martinson, D.G., McIntyre, A., Mix, A.C., Molfino, B., Morley, J.J., Peterson, L.C., Pesias, N.G., Prell, W.L., Raymo, M.E., Shackleton, N.J., Toggweiler, J.R., 1992. On the structure and origin of major glaciation cycles. pt. 1, linear responses to Milankovitch forcing. Paleoceanography 7, 701–738.
Isaac, G.L. (Ed.), 1997. Koobi Fora Research Project, Volume 5 Plio-Pleistocene Archaeology. Clarendon Press, New York. 596 pp.
Jenny, H., 1980. The soil resource: origin and behavior. Springer Verlag, New York.
Johanson, D.C., Taieb, M., Coppens, Y., 1982. Pliocene hominids from the Hadar Formation, Ethiopia (1973–1977): stratigraphic, chronologic, and paleoenvironmental contexts, with notes on hominid morphology and systematics. American Journal of Physical Anthropology 57, 373–402.
Katoh, S., Nagaoka, S., WoldeGabriel, G., Renne, P., Snow, M.G., Beyene, Y., Suwa, G., 2000. Chronostratigraphy and correlation of the Plio-Pleistocene tephra layers of the Konso Formation, southern Main Ethiopian Rift, Ethiopia. Quaternary Science Reviews 19, 1305–1317.
Keeling, C.D., Mook, W.G., Tans, P.P., 1979. Recent trends in the $^{13}C/^{12}C$ ratio of atmospheric carbon dioxide. Nature 277, 121–123.
Kim, S.-T., O'Neil, J.R., 1997. Equilibrium and nonequilibrium oxygen isotope effects in synthetic carbonates. Geochimica et Cosmochimica Acta 61, 3461–3475.
Kimbel, W.H., Johanson, D.C., Rak, Y., 1994. The first skull and other new discoveries of *Australopithecus afarensis* at Hadar, Ethiopia. Nature 368, 449–451.
Kimbel, W.H., Walter, R.C., Johanson, D.C., Reed, K.E., Aronson, J.L., Assefa, Z., Marean, C. W., Eck, G.G., Bobe, R., Hovers, E., Rak, Y., Vondra, C.F., Yemane, T., York, D., Chen, Y., Evenson, N.M., Smith, P.E., 1996. Late Pliocene *Homo* and Oldowan tools from the Hadar Formation (Kada Hadar Member), Ethiopia. Journal of Human Evolution 31, 549–561.
Lambers, H., Chapin, F.S., Pons, T.L., 2008. Plant Physiological Ecology. Springer, New York.
Leakey, M.G., Leakey, R.E., 1978. The Fossil hominids and an introduction to their context, 1968–1974. Koobi Fora Research Project, 1. Clarendon Press, New York. 191 pp.
Lepre, C.J., Quinn, R.L., Joordens, J.C.A., Swisher, C.C., Feibel, C.S., 2007. Plio-Pleistocene facies environments from the KBS Member, Koobi Fora Formation: implications for climate controls on the development of lake-margin hominin habitats in the northeast Turkana Basin (northwest Kenya). Journal of Human Evolution 53, 504–514.
Levin, N.E., Quade, J., Simpson, S.W., Semaw, S., Rogers, M.J., 2004. Isotopic evidence for Plio-Pleistocene environmental change at Gona, Ethiopia. Earth and Planetary Science Letters 219, 93–110.
Levin, N.E., Zipser, E.J., Cerling, T.E., 2009. Isotopic composition of waters from Ethiopia and Kenya: insights into moisture sources for eastern Africa. Journal of Geophysical Research 114, D23306.
Liutkus, C.M., Wright, J.D., Ashley, G.M., Sikes, N.E., 2005. Paleoenvironmental interpretation of lake-margin deposits using delta C-13 and delta O-18 results from early Pleistocene carbonate rhizoliths, Olduvai Gorge, Tanzania. Geology 33, 377–380.
Machette, M.N., 1985. Calcic soils of the southwestern United States. Geological Society of America, Special Papers 203, 1–21.
McDougall, I., Brown, F.H., 2006. Precise $^{40}Ar/^{39}Ar$ geochronology for the upper Koobi Fora Formation, Turkana Basin, northern Kenya. Journal of the Geological Society of London 163, 205–220.
McDougall, I., Brown, F.H., 2008. Geochronology of the pre-KBS Tuff sequence, Omo Group, Turkana Basin. Journal of the Geological Society of London 165, 549–562.
McDougall, I., Brown, F.H., Fleagle, J.G., 2005. Stratigraphic placement and age of modern humans from Kibish, Ethiopia. Nature 433, 733–736.
Nordt, L.C., Wilding, L.P., Lynn, W.C., Crawford, C.C., 2004. Vertisol genesis in a humid climate of the coastal plain of Texas, U.S.A. Geoderma 122, 83–102.
Passey, B.H., Levin, N.E., Cerling, T.E., Brown, F.H., Eiler, J.M., 2010. High-temperature environments of human evolution in East Africa based on bond ordering in paleosol carbonates. Proceedings of the National Academy of Sciences U. S. A. 107, 11245–11249.
Quade, J., Cerling, T.E., 1995. Expansion of C_4 grasses in the Late Miocene of Northern Pakistan: evidence from stable isotopes in paleosols. Palaeogeography, Palaeoclimatology, Palaeoecology 115, 91–116.
Quade, J. and Levin, N.E., in press. East African hominid paleoecology: isotopic evidence from paleosols, in: M. Sponheimer, K. Reed, J. Lee-Thorp and P. Ungar (Eds.), Early Hominin Paleoecology. University of Colorado Press.
Quade, J., Cerling, T.E., Bowman, J.R., 1989. Systematic variations in the carbon and oxygen isotopic composition of pedogenic carbonate along elevation transects in the southern Great Basin, United States. Geological Society of America Bulletin 101, 464–475.
Quade, J., Levin, N., Semaw, S., Stout, D., Renne, P.R., Rogers, M., Simpson, S., 2004. Paleoenvironments of the earliest stone toolmakers, Gona, Ethiopia. Geological Society of America Bulletin 116, 1529–1544.
Quade, J., Levin, N.E., Simpson, S.W., Butler, R.F., McIntosh, W., Semaw, S., Kleinsasser, L., Dupont-Nivet, G., Renne, P., Dunbar, N., 2008. The Geology of Gona, Afar, Ethiopia. In: Quade, J., Wynn, J.G. (Eds.), The Geology of Early Humans in the Horn of Africa: Geological Society of America Special Paper, 446, pp. 1–31.
Quinn, R.L., Lepre, C.J., Wright, J.D., Feibel, C.S., 2007. Paleogeographic variations of pedogenic carbonate $\delta^{13}C$ values from Koobi Fora, Kenya: implications for floral compositions of Plio-Pleistocene hominin environments. Journal of Human Evolution 53, 560–573.
Retallack, G.J., 2005. Pedogenic carbonate proxies for amount and seasonality of precipitation in paleosols. Geology 33, 333–336.
Romanek, C.S., Grossman, E.L., Morse, J.W., 1992. Carbon isotopic fractionation in synthetic aragonite and calcite: effects of temperature and precipitation rate. Geochimica et Cosmochimica Acta 56, 419–430.
Rozanski, K., Araguas-Araguas, L., and Gonfiantini, R., 1996. Isotope patterns of precipitation in the East African region. In: Johnson, T.C., Odada, E.O. (Eds.), The Limnology, Climatology and aleoclimatology of the East African Lakes. Gordon & Breach, Amsterdam, pp. 79–93.
Semaw, S., Renne, P., Harris, J.W.K., Feibel, C.S., Bernor, R.L., Fesseha, N., Mowbray, K., 1997. 2.5-million-year-old stone tools from Gona, Ethiopia. Nature 385, 333–336.
Sepulchre, P., Ramstein, G., Fluteau, F., Schuster, M., Tiercelin, J.-J., Brunet, M., 2006. Tectonic uplift and eastern Africa aridification. Science 311, 1419–1423.
Sikes, N.E., Ashley, G.M., 2007. Stable isotopes of pedogenic carbonates as indicators of paleoecology in the Plio-Pleistocene (upper Bed I), western margin of the Olduvai Basin, Tanzania. Journal of Human Evolution 53, 574–594.
Simpson, S.W., Quade, J., Levin, N.E., Butler, R., Dupont-Nivet, G., Everett, M., Semaw, S., 2008. A female *Homo erectus* pelvis from Gona, Ethiopia. Science 322, 1089–1092.
Tieszen, L.L., Senyimba, M.M., Imbamba, S.K., Troughton, J.H., 1979. The distribution of C_3 and C_4 grasses and carbon isotope discrimination along an altitudinal and moisture gradient in Kenya. Oecologia 37, 337–350.
Tipple, B.J., Meyers, S.R., Pagani, M., 2010. Carbon isotope ratio of Cenozoic CO_2: a comparative evaluation of available geochemical proxies. Paleoceanography 25, PA3202.
Trauth, M.H., Maslin, M.A., Deino, A.L., Strecker, M.R., Bergner, A.G.N., Dühnforth, M., 2007. High- and low-latitude forcing of Plio-Pleistocene East African climate and human evolution. Journal of Human Evolution 53, 475–486.
van der Merwe, N.J., 1991. The canopy effect, carbon isotope ratios and foodwebs in Amazonia. Journal of Archaeological Science 18, 249–259.
White, T.D., Asfaw, B., Beyene, Y., Haile-Selassie, Y., Lovejoy, C.O., Suwa, G., WoldeGabriel, G., 2009. *Ardipithecus ramidus* and the Paleobiology of Early Hominids. Science 326, 64.
WoldeGabriel, G., Hart, W.K., Katoh, S., Beyene, Y., Suwa, G., 2005. Correlation of Plio-Pleistocene Tephra in Ethiopian and Kenyan rift basins: temporal calibration of geological features and hominid fossil records. Journal of Volcanology and Geothermal Research 147, 81–108.

Wynn, J.G., 2000. Paleosols, stable carbon isotopes, and paleoenvironmental interpretation of Kanapoi, northern Kenya. Journal of Human Evolution 39, 411–432.
Wynn, J.G., 2004. Influence of Plio-Pleistocene aridification on human evolution: evidence from paleosols of the Turkana Basin, Kenya. American Journal of Physical Anthropology 123, 106–118.
Wynn, J.G., Alemseged, Z., Bobe, R., Geraads, D., Reed, D., Roman, D.C., 2006. Geological and palaeontological context of a Pliocene juvenile hominin at Dikika, Ethiopia. Nature 443, 332–336.
Wynn, J.G., Roman, D.C., Alemseged, Z., Reed, D., Geraads, D., Munro, S., 2008. Stratigraphy, depositional environments, and basin structure of the Hadar and Busidima Formation at Dikika, Ethiopia. In: Quade, J., Wynn, J.G. (Eds.), The Geology of Early Humans in the Horn of Africa. : Geological Society of America Special Paper, 446. The Geological Society of America, Boulder, pp. 87–118.
Young, H.J., Young, T.P., 1983. Local distribution of C_3 and C_4 grasses in sites of overlap on Mount Kenya. Oecologia 58, 373–377.